

# **DASM-T: Delta ANN Simulation Model for Turbidity, Phase 1 Results**



Photo Credit: Dave Giordano  
Ecositemedia.com

© The Regents of the University of California  
Source: University of California ANR

*Prepared for:*  
**Paul Hutton, Ph.D., P.E.**  
**Metropolitan Water District of Southern California**  
**1121 L Street, Suite 900**  
**Sacramento, CA 95814-3974**

*Prepared by:*



**Limin Chen and Sujoy B. Roy**  
**Tetra Tech, Inc.**  
**3746 Mt. Diablo Blvd, Suite 300**  
**Lafayette, CA 94549-3681**

**August 8, 2012**



# TABLE OF CONTENTS

---

<b>1</b>	<b>Introduction .....</b>	<b>1-1</b>
<b>2</b>	<b>Approach .....</b>	<b>2-1</b>
2.1	Overall Approach.....	2-1
2.2	DSM2 Model.....	2-1
2.2.1	DSM2 Turbidity Model.....	2-1
2.2.2	Formulation of Boundary Condition Scenarios .....	2-2
2.3	Artificial Neural Network Model.....	2-5
2.3.1	Model Inputs .....	2-5
2.3.2	ANN Output Locations .....	2-7
2.3.3	ANN Model Structure .....	2-8
2.3.4	Training Approach.....	2-11
2.3.5	ANN Model Simulation and Validation.....	2-11
<b>3</b>	<b>Results .....</b>	<b>3-1</b>
3.1	DSM2 Simulated Turbidity at Target Locations .....	3-1
3.2	Ann Training Results .....	3-4
3.3	Training With Tidal Effects.....	3-13
3.4	Evaluation of Single ANN Model Versus Seven Separate Models .....	3-22
3.5	Evaluation of Alternative Network Structure.....	3-22
3.6	Validation Against Historical Dataset .....	3-24
<b>4</b>	<b>Summary and Discussion.....</b>	<b>4-1</b>
<b>5</b>	<b>References.....</b>	<b>5-1</b>
	<b>Appendix A: Flow-Turbidity Relationships at Boundary Locations .....</b>	<b>A-1</b>
	Sacramento River at Freeport .....	A-1
	San Joaquin River at Vernalis .....	A-2
	Yolo Bypass .....	A-2
	Cosumnes River.....	A-3
	Mokelumne River .....	A-3
	Calaveras River.....	A-3
	<b>Appendix B: Comparison of DSM2 Output to Real-Time Turbidity Data Collected in the Delta.....</b>	<b>B-1</b>
	<b>Appendix C: Time Series of Trained and DSM2 Simulated Turbidity for the Training, Validation and Test Datasets for: a) Twelve Scenarios; b) 20-year; c) 5-year; and d) 1-year Period of Scenario 5.....</b>	<b>C-1</b>

**Appendix D: ANN Trained Turbidity Using 12 Scenarios Compared to DSM2  
Simulated Turbidity..... D-1**

# ACRONYMS

---

ANN	Artificial Neural Network
CDEC	California Data Exchange Center
CVP	Central Valley Project
DSM2	Delta Simulation Model II
MWD	Municipal Water District
NCD	Net Channel Depletions
OMR	Old and Middle River
SWP	State Water Project



# 1 INTRODUCTION

---

The Delta smelt (*Hypomesus transpacificus*) is an endangered species endemic to the Sacramento-San Joaquin estuary of California, with low recorded abundance in the last decade by the Interagency Ecological Program. A 2008 Biological Opinion by the U.S. Fish and Wildlife Service recommended changes in the manner in which flows and freshwater exports through the Delta are managed to address the decline in population of this species (<http://www.fws.gov/sfbaydelta/ocap/>). Delta smelt abundance is related to various water quality parameters, including temperature, conductivity, and turbidity. Possibly due to linkages between Delta smelt migration and turbidity levels (Armor and Sommer, 2006), California Department of Water Resources scientists have observed that there is an increase in Delta smelt salvage at the water export facilities when the turbidity exceeds a level of approximately 12 nephelometric turbidity units (NTU).

To support implementation of the 2008 Biological Opinion, there is a need to understand and predict fate and movement of turbidity in the Delta. Besides greater collection of turbidity data that has been initiated since 2009, turbidity modeling is also needed. Two such approaches include mechanistic modeling using the Delta Simulation Model (DSM-2) (Liu and Sandhu, 2011) and using the Resource Management Associates RMA-2 model (RMA, 2008). These models compute turbidity within the Delta channels given inputs of flow and turbidity at all relevant boundaries. However, both modeling approaches require considerable user expertise and computational time to run, hence limiting their accessibility. There is an additional need for a tool that can be used to provide rapid predictions of turbidity in two situations: for near-term operations planning, where there is a need to estimate turbidity expected in the following days under a variety of possible operating scenarios, and, for long-term water supply planning, where there is a need to estimate turbidity-related export constraints in water operations models (e.g. CalSim) run over multi-year periods. Under these conditions, running a fully mechanistic model of the system is generally not computationally feasible.

To fit this need for generating rapid predictions, Artificial Neural Networks (ANNs) were proposed as an alternative mathematical approach to conventional statistical methods and

mechanistic models. ANNs use simple elements (neurons) and connections between elements using a range of functional forms to represent complex real-world data. The ANN methodology was inspired by biological nervous systems (Demuth and Beale, 2002) and has found broad application in the prediction and control of complex systems. An ANN can be trained to perform a particular function through adjusting values that form the connections between elements (weights). In this context, the term training is analogous to parameter estimation used in statistical and mechanistic models. ANNs offer several advantages over alternative statistical methods: 1) they can include non-linear functions and represent a broad range of functional forms, and 2) they can be set up to approximate relatively complex problems, such as the hydrodynamics in the Delta. In recent years, ANNs have also become popular in the water resources field: recent literature reviews identified more than 300 peer-reviewed applications of ANNs to water resources problems worldwide (Maier and Dandy, 2000; Maier et al., 2010). Although the majority of applications of ANNs to water resources are related to flow, some applications have focused on water quality (e.g., salinity, nitrate, sediment; Maier et al. 2010).

The ANN approach has been used broadly in the Sacramento–San Joaquin Delta in predicting salinity at various interior locations by the California Department of Water Resources (DWR) (Finch and Sandhu, 1995; Sandhu et al., 1999) and impacts of sea level rise (Seneviratne et al., 2008). The delta salinity ANN model has been integrated into the state-wide operations model CalSim (Wilbur and Munevar, 2001). The salinity ANN is trained on DSM2 results that may represent historical or future conditions, through taking into account individual flow components and operational parameters as model inputs. In this sense, the ANN model has the advantage as previous approaches are based on historical measurements alone and cannot account for potential future changes in the Delta hydrology. The current version of DWR’s ANN model predicts flow-salinity relationships at nine locations in the Delta including Emmaton, Jersey Point, Old River at Rock Slough, Collinsville, Chipps Island, Antioch, Central Valley Project intake (Jones pumping plant), Clifton Court Forebay intake (Banks pumping plant), and Los Vaqueros intake at Old River. This version of the ANN model also calculates the position of X2 in the estuary (location corresponding to a salinity of 2 parts per thousand at the bottom of the water column).

The goal of this study was to explore the potential of developing a Delta ANN turbidity model, representing historical or future potential conditions within the Delta. Because the underlying turbidity data through the Delta are only available for a relatively brief time window (from 2009 to present), this study used model-calculated turbidity values for the training of the ANN. As it is well known that ANNs (and most data-driven empirical approaches) perform best at interpolating within conditions that have been used for training and perform poorly at extrapolating beyond the training range, a key objective of this work was to generate a wide range of model inputs to create a broad range of data for training. DSM2 was run with multiple turbidity boundary inputs, with a 20-year

hydrologic time series, and was used to create the dataset that was be used for training/validating the ANN. The present analysis, and resulting model, termed DASM-T for Delta ANN Simulation Model-Turbidity, is termed a Phase 1 study because the goal was to demonstrate whether ANNs could indeed successfully replicate turbidity in the Delta, with possible extensions of the ANN approach based on the results of this study.



## 2 APPROACH

---

### 2.1 OVERALL APPROACH

The overall approach used in developing the Delta ANN turbidity model was to train the model based on a set of boundary scenarios formulated to represent historical or potential future conditions in the Delta, with model inputs generated by the DSM2 model, described below. The DSM2 model was selected to simulate flow and turbidity relationships within the Delta, rather than using the observed data directly. This is because DSM2 is able to mechanistically simulate the response in turbidity at different Delta locations, in response to changes in individual flow components and operation parameters that could potentially occur in the future. This feature may not be captured by using observed turbidity data available today, which span a relatively short time frame. Given the constraint with the availability of observed data, the DSM2 model outputs are considered the next best option for developing a long-term data set that is able to account for future changes in Delta flow and operation under a range of hydrologic conditions.

### 2.2 DSM2 MODEL

The DSM2 model is a one-dimensional hydrodynamic and water quality model that dynamically simulates hydrodynamics, water quality and particle tracking in a network of riverine or estuarine channels with Delta (DWR, 2002). DSM2 calculates flow, stage, velocity, mass transport processes for conservative and non-conservative constituents, including (but not limited to) salinity, water temperature, dissolved organic carbon, nutrients, dissolved oxygen, and transport of individual neutrally-buoyant particles. DSM2 is a powerful tool for analysis of complex hydrodynamic, water quality, and ecological conditions, and has a long history of use within DWR to address various flow and water quality problems.

#### 2.2.1 DSM2 TURBIDITY MODEL

A recent version of the DSM2 model was used to simulate turbidity within the Delta (Liu and Sandhu, 2011). In this application, turbidity was simulated as a constituent governed by advection-dispersion with first-order decay/loss due to settling. The model was

calibrated for the wet season of 2010, using detailed turbidity data available at a number of locations at 15-minute intervals, and using variable decay rates through the Delta (varying in space, but constant in time). The calibrated DSM2 model is considered appropriate for the use here because: 1) the model was calibrated for high flow time periods when the dominant source of turbidity is the watershed derived inputs; 2) the model is calibrated for a time period for a typical adult delta smelt pre-spawning period of approximately December through February. Model-simulated turbidity at 15-minute intervals and daily average values compared well with observed values at a number of locations including the Sacramento River at Rio Vista, Decker Island, Prisoner's Point, Holland Cut, San Joaquin River at Jersey Point, Garwood, Mossdale, Brandt Bridge, and Old River at Bacon Island, and Victoria Canal.

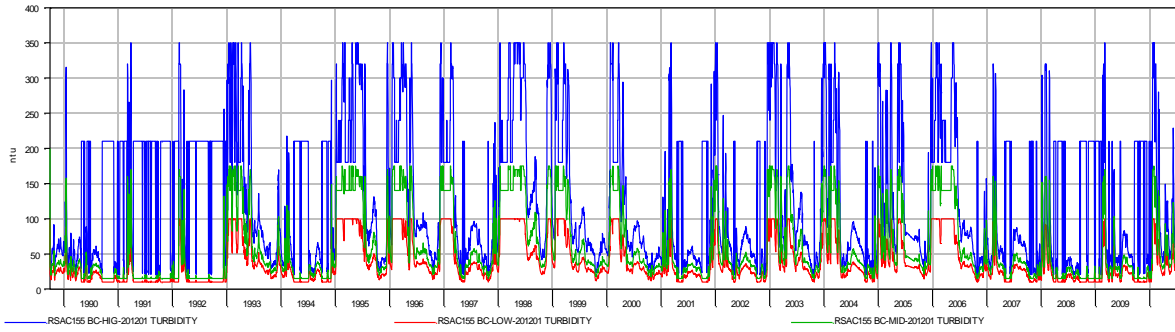
### **2.2.2 FORMULATION OF BOUNDARY CONDITION SCENARIOS**

The calibrated DSM2 turbidity model (Liu and Sandhu, 2011) was used for simulating flow and turbidity relationships within the Delta under a set of formulated boundary scenarios. The DSM2 model was run for a period of 20 years from 1990–2010. The formulated boundary scenarios take into account combinations of different turbidity levels (low, middle, and high levels) from three sources: North Delta (Sacramento River+Yolo), San Joaquin River, and east side tributaries (Mokelumne, Cosumnes, and Calaveras Rivers). Turbidity from Delta Islands and Martinez locations were set as constants. The boundary scenarios also considered the effect of south Delta diversions (SWP and CVP). A total of 12 scenarios were formulated (Table 2-1). The model was run under the assumptions that: 1) the DCC gate is closed during all months; 2) south Delta temporary barriers are not installed. The assumption is reasonable given that the ANN model is expected to be used for December through February periods. Detailed flow-turbidity relationships used to determine boundary turbidity inputs under low, middle or high turbidity conditions at different boundary locations are listed in Appendix A. The derived boundary conditions for the low, middle and high turbidity levels are shown graphically in Figure 2-1.

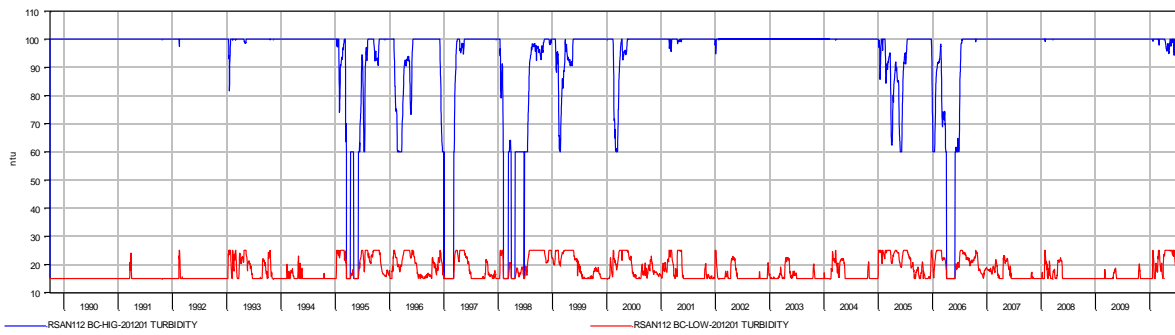
**Table 2-1**  
**DSM2 Simulations and Associated Turbidity**  
**Boundary Conditions Used for Generating ANN Training Data**

Run	Hydrology	Sacramento	SJR	Yolo	Cosumnes	Mokelumne	Calaveras	Islands	Martinez
1	Historical	Low	Low	Low	Low	Low	Low	10 ntu	26.6 ntu
2	Historical	Mid	Low	Mid	Mid	Mid	Mid	10 ntu	26.6 ntu
3	Historical	High	Low	High	High	High	High	10 ntu	26.6 ntu
4	Historical	Low	High	Low	Low	Low	Low	10 ntu	26.6 ntu
5	Historical	Mid	High	Mid	Mid	Mid	Mid	10 ntu	26.6 ntu
6	Historical	High	High	High	High	High	High	10 ntu	26.6 ntu
7	Historical w/o Exports	Low	Low	Low	Low	Low	Low	10 ntu	26.6 ntu
8	Historical w/o Exports	Mid	Low	Mid	Mid	Mid	Mid	10 ntu	26.6 ntu
9	Historical w/o Exports	High	Low	High	High	High	High	10 ntu	26.6 ntu
10	Historical w/o Exports	Low	High	Low	Low	Low	Low	10 ntu	26.6 ntu
11	Historical w/o Exports	Mid	High	Mid	Mid	Mid	Mid	10 ntu	26.6 ntu
12	Historical w/o Exports	High	High	High	High	High	High	10 ntu	26.6 ntu

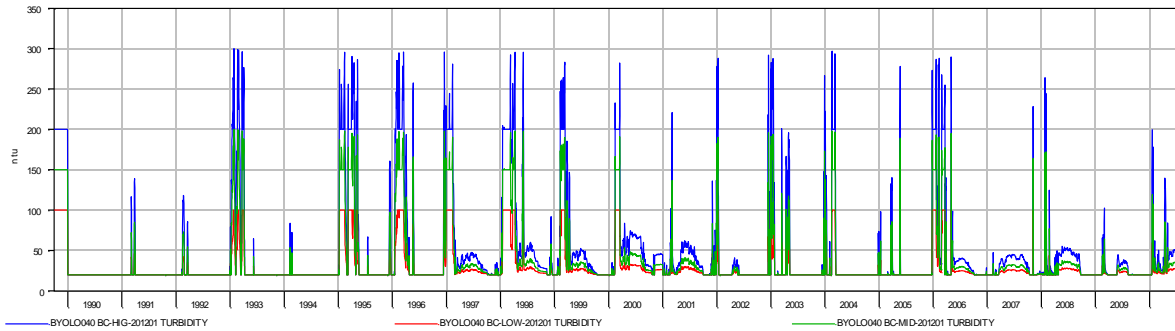
a. Sacramento River



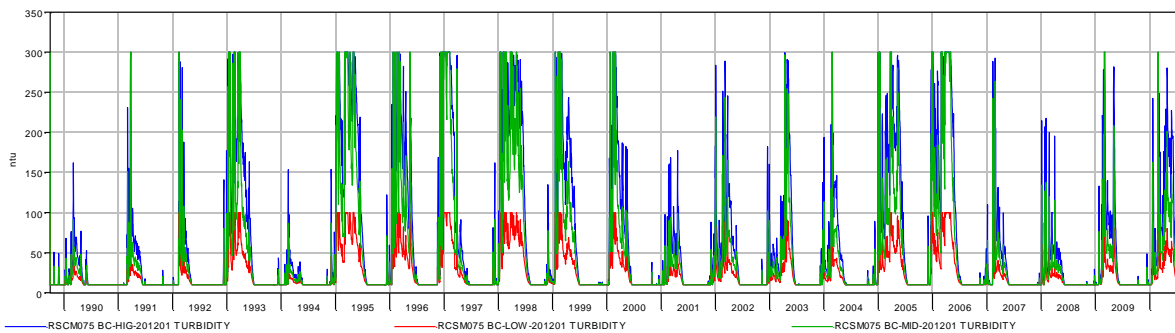
b. San Joaquin River



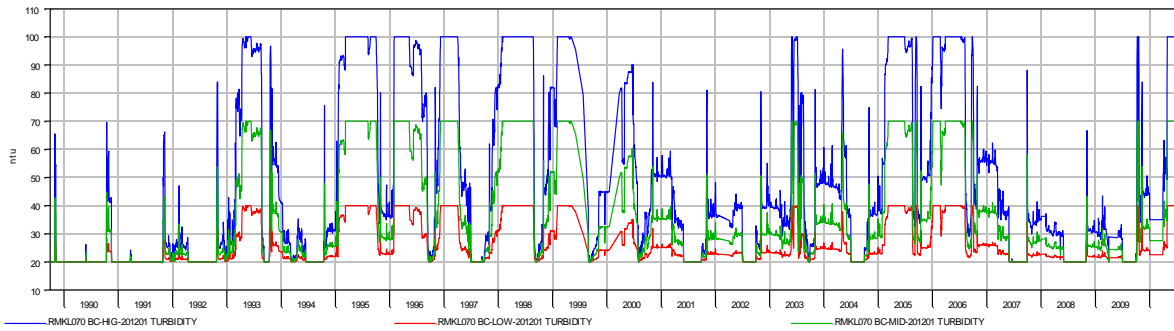
c. Yolo Bypass



d. Cosumnes River



e. Mokelumne River



f. Calaveras River

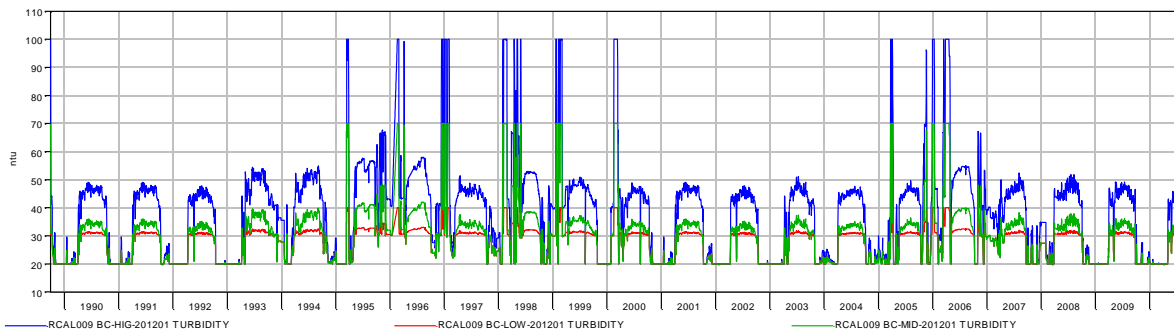


Figure 2-1 Boundary conditions of low, middle, and high turbidity levels at: a) Sacramento River; b) San Joaquin River; c) Yolo Bypass; d) Cosumnes; e) Mokelumne, and f) Calaveras Rivers.

## 2.3 ARTIFICIAL NEURAL NETWORK MODEL

### 2.3.1 MODEL INPUTS

For the ANN model training, a set of six input variables were used. These input variables were considered to be the main boundary conditions that influence turbidity dynamics within Delta. These inputs include three flow and three turbidity variables. The three flow inputs are: north Delta inflow, east side stream inflow, and calculated Old and Middle River (OMR) flow. Three turbidity inputs are north Delta turbidity, east side stream turbidity, and San Joaquin River (Vernalis) turbidity.

#### 2.3.1.1 NORTH DELTA INFLOW

The north Delta inflow was calculated as the total of the Sacramento River and Yolo Bypass inflow. Observed daily flow records from the Sacramento River at Freeport and Yolo Bypass flow from DSM2 for the period of 1990–2010 were used in formulating the ANN input time series of this variable, originally obtained from DAYFLOW of IEP (<http://www.water.ca.gov/dayflow/output/index.cfm>).

### 2.3.1.2 EAST SIDE STREAM INFLOW

The East Side stream flow was calculated as total of inflow from the Mokelumne River, the Cosumnes River and the Calaveras River. Daily flow records for the period of 1990–2010 at these locations from DSM2 were derived from DSM2 inputs, compiled by DWR, originally obtained from DAYFLOW of IEP, (<http://www.water.ca.gov/dayflow/output/index.cfm>).

### 2.3.1.3 OLD AND MIDDLE RIVER (OMR) FLOW

As found in previous work, there is a correlation between adult Delta smelt salvage at the CVP-SWP export pumps and the combined OMR flows near Bacon Island (Smith et al., 2006). Several hydraulic forces determine the volume and direction of flows at these locations. The key hydraulic forces include: San Joaquin River flows entering the head of Old River, water diversions from the south Delta, and tides. The empirical OMR flow model implemented in the CalSim model was used; this model is calibrated with data generated by DWR's DSM2 and validated with field observations (Hutton, 2008). A south Delta water balance was used in determining OMR flows:

OMR flow = San Joaquin River flow at Vernalis

- + Indian Slough flow at Old River
- San Joaquin River flow downstream of HOR
- Clifton Court Forebay diversions
- Jones pumping plant diversions
- CCWD Old River intake diversions
- South Delta net channel depletion

The above water balance was used in calculating OMR flow for ANN input. DSM2 boundary conditions were used for San Joaquin River flows at Vernalis, diversions at Jones Pumping Plant and CCWD Old River intake (Hutton, 2008). Computed data from DWR's Delta Island Consumptive Use (DICU) model were used in the water balance for south Delta net channel depletions. DSM2 simulated data were used in water balance calculation for flows at Indian Slough at Old River, San Joaquin River downstream of HOR (Head of Old River) and diversions at Clifton Court Forebay. The data used to compute the south Delta water balance are listed in Table 2-2.

**Table 2-2**  
**DSM2 data used in OMR flow calculation Hutton (2008)**

<b>Data Type</b>	<b>Data Location</b>	<b>Observed or Computed</b>
River Flow	Old River at Bacon Island	Computed
River Flow	Middle River at Bacon Island	Computed
River Flow	San Joaquin River at Vernalis	Observed
River Flow	Indian Slough at Old River	Computed
River Flow	San Joaquin River d/s HOR	Computed
Diversion	Clifton Court Forebay	Computed
Diversion	Jones Pumping Plant	Observed
Diversion	CCWD Intake at Old River	Observed
Diversion	South delta net channel depletions	Computed

#### 2.3.1.4 NORTH DELTA TURBIDITY

The north Delta turbidity was calculated as flow-weighted averages of turbidities at the Sacramento River at Freeport and Yolo Bypass. Turbidities at Sacramento River at Freeport and Yolo Bypass were computed based on flow and turbidity relationships derived from an analysis (outlined in Appendix A) for low, mid and high turbidity input levels (RMA, 2010; Hutton, personal communication). The flow records used to derive turbidity inputs are observed values used in the DSM2 inputs.

#### 2.3.1.5 EAST SIDE STREAM TURBIDITY

The east side stream turbidity was calculated as flow weighted averages of turbidities at the Mokelumne, Cosumnes, and Calaveras Rivers. Turbidities at these tributaries were computed based on flow and turbidity relationships derived from an analysis (outlined in Appendix A) for low, middle and high turbidity input levels (RMA, 2010). The flow records for derive turbidity inputs are observed values used in the DSM2 inputs.

#### 2.3.1.6 VERNALIS TURBIDITY

Turbidity from San Joaquin River at Vernalis was computed based on flow-turbidity relationships derived from an analysis (outlined in Appendix A) for low, middle and high turbidity input levels (RMA, 2010). The flow records for deriving turbidity inputs are observed values used in the DSM2 inputs.

### 2.3.2 ANN OUTPUT LOCATIONS

The DSM2 model simulates turbidity at locations throughout the Delta, a subset of which were used for this work. DSM2 output at 15-minute intervals was used to compute daily averages for the ANN training. DSM2 simulations of turbidity at these selected locations were used in training and for developing the Delta turbidity ANN model. The model was focused on turbidity at seven locations of interest (Figure 2-2):

- Sacramento River at Rio Vista
- Old River at Bacon Island
- Old River at Quimby Island
- San Joaquin River at Prisoner’s Point
- Middle River at Holt
- Clifton Court Forebay Entrance
- Victoria Canal at Byron

The training data set consisted of values over a 20-year hydrologic period for 12 boundary conditions, representing 365x20x12 (=87,600) data points for each output location.

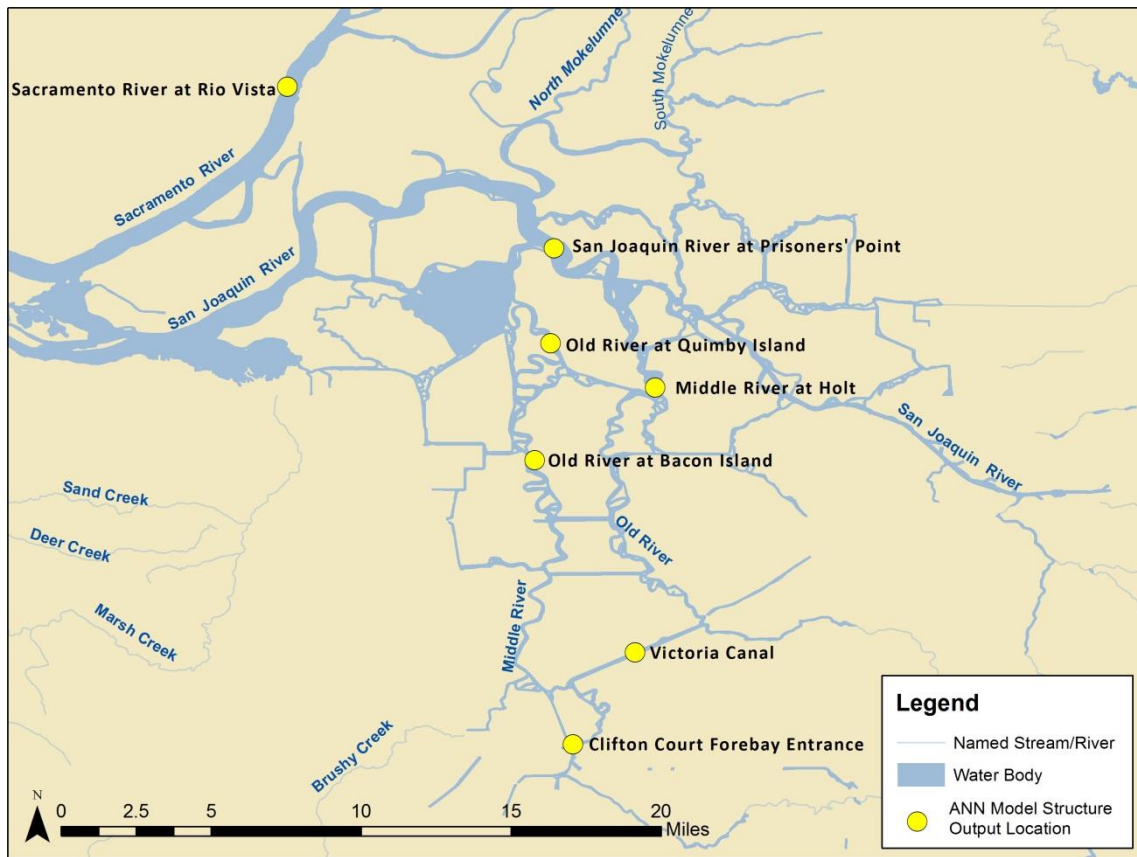


Figure 2-2 Map of the Delta showing the stations used for ANN output. Values at these stations were obtained from DSM2 runs for 12 boundary scenarios.

### 2.3.3 ANN MODEL STRUCTURE

The ANN architectures in common use have been divided into feed-forward and recurrent networks (Maier et al. 2010). The feed-forward network propagates information in one direction, from input layer to output layer. The recurrent network propagates information not only in one direction, but also has a feedback loop to feed information to

previous layer or the same layer. There are several types of feed-forward network architectures, including Multilayer Perceptrons (MLPs), Generalized Regression Neural Networks (GRNNs), Radial Basis Function (RBF) networks, Neurofuzzy networks and support vector machine (SVMs).

An MLP is the most commonly used architecture employing three or more layers with linear or non-linear functions. The input layer simply passes on the weighted inputs to the subsequent layer. The use of non-linear functions at the hidden and output layers provides the capability to model complex systems with non-linearity. A GRNN is able to approximate any function using input and output, which consists of four layers, an input layer, a pattern layer, a summation layer, and an output layer. GRNNs do not rely on training but use a standard statistical technique called kernel regression for deriving weights. RBF networks are similar to MLPs. The major difference is that the hidden layer neurons are specified by radial basis functions and output layer neurons uses linear activation functions. The neurofuzzy networks are based on an integration of neural networks and fuzzy logic. SVMs are machine learning algorithms in which the risk of prediction error and risk associated with model structure are minimized simultaneously.

Recently, recurrent or auto-regressive networks, i.e., networks with internal feedbacks, have been proposed as alternatives to feed-forward networks. In this case the model output (or predicted values) can be fed back into the model input with a time lag. Feed-forward networks may also be considered as special cases of recurrent networks. Feed-forward networks require dynamic systems to be treated explicitly, which is achieved through specifying time lagged inputs. Recurrent networks model dynamic properties implicitly. However, it has been found that recurrent networks have difficulties in capturing long-term dependencies. The nonlinear autoregressive network with exogenous inputs (NARX) recurrent network, which uses an explicit time lag, is considered to be an improvement over traditional recurrent networks, and may be considered for the present application.

The dynamic nature of flow and turbidity in the Delta requires a network structure that takes into account the time-series effect. Although other network structures may receive increasing attention in the recent literature, the MLPs are by far the most popular network structure used in water resources applications to date, representing more than 90% of peer-reviewed applications in the water resources field (Maier et al. 2010). For this reason, the feed-forward MLP network was selected in this study, and is shown schematically in Figure 2-3. In this network, the input layer, termed  $x(t)$  contains time series of six input variables (3 flow inputs, and 3 turbidity inputs as described earlier). The hidden layer uses 15 neurons, which is formulated based on input variables using a set of weights ( $W$ ) and biases ( $b$ ). For 15 neurons and 6 input variables, this will yield a total of 90 weights and 90 bias parameters that need to be adjusted during training. An input time delay of 1–4 days can be used, each with its own set of weights and bias parameters. For a time delay of 2 days, the network will yield 180 weights and 180 bias

parameters. The output layer,  $y(t)$ , contains seven output variables. The hidden layer is converted to the output layer through another set of weights and biases.

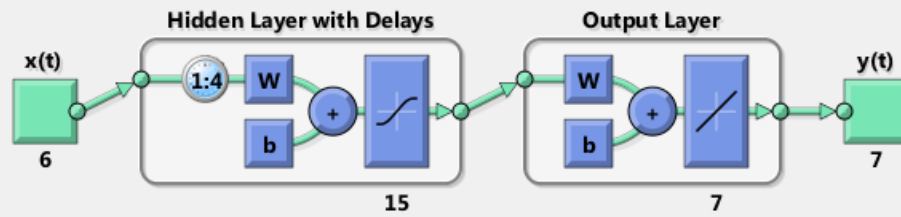


Figure 2-3 Feed-forward ANN model structure (inputs = 6 boundaries (3 flow + 3 turbidity), hidden neurons = 10; time delay = 1–4 days; outputs: turbidity at 7 locations).  $x(t)$  represents the input,  $y(t)$  the output, and  $W$  and  $b$  represents the weights and biases.

The network structure, together with the model architecture, defines the functional relationships between the input layer and the output layer. The structure, specifically the number of neurons and the time lag is determined through varying network size and time of delay to determine network configuration that provides the highest correlation between the predicted and observed results. This is basically a trial and error approach and is widely used in training of similar data sets (Maier et al., 2010). For the current application, the ANN model was implemented using the Neural Network Toolbox, an add-on package in the Matlab programming environment (Beale et al., 2011). Through testing across a wide range of network sizes and time delays, an optimal size and of time delay was found, when correlations between ANN and DSM2 simulated turbidity were the highest.

In addition to the feed-forward network, which was the primary focus of this study, the quality of the fit was also compared to that obtained from the NARX recurrent network, where the output of the model at the previous time steps is also used as an input as shown on the left side of Figure 2-4. The NARX network training can be implemented in what is termed the “open loop” mode, where the output data are used for training. Once the model is trained, it can be converted to a “closed loop,” where the values of  $y(t)$  on the left side are obtained from ANN for the previous time step.

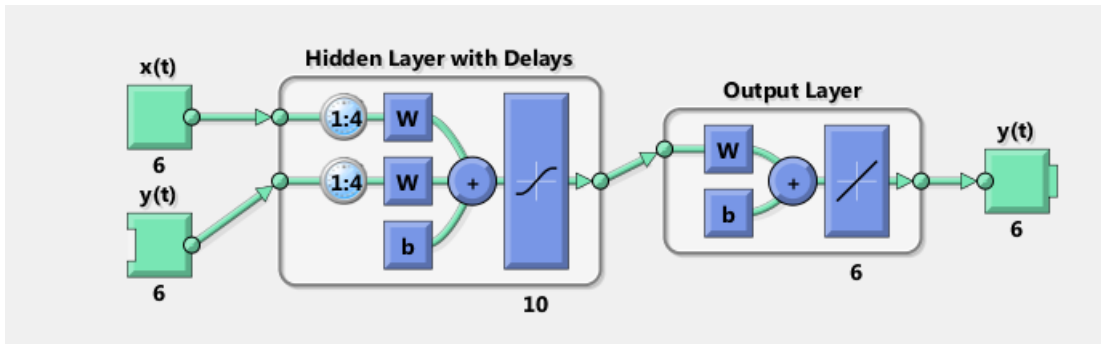


Figure 2-4 Matlab NARX ANN model structure ( $y(t) = f(x(t-1), \dots, x(t-d))$ ); inputs = 6 boundaries (3 flow + 3 turbidity), hidden neurons = 10; time delay = 1–4 days; outputs: turbidity at 7 locations). During training,  $y(t)$  on the left side can be approximated by the training data (termed “open loop”), and during testing,  $y(t)$  can be replaced by the ANN predicted value (termed “closed loop”).

### 2.3.4 TRAINING APPROACH

The majority of the ANN calibration approaches is deterministic, through determination of a single parameter vector that minimizes an error measure between predicted and observed values (Maier et al. 2010). This approach was employed in the present study. Two general types of deterministic optimization approaches exist: the global optimization and the local optimization. The local methods are prone to becoming trapped in local optima if the error surface is rugged, however they are generally computationally more efficient. The local methods rely on gradient information, through first-order methods (e.g., back-propagation) or second-order methods (e.g., Newton’s method). Global optimization methods, such as genetic algorithms, have better ability to find global optima in error surface however are less computationally efficient. Therefore for the ANN training, the back-propagation (Levenberg-Marquardt back-propagation) method is commonly used.

### 2.3.5 ANN MODEL SIMULATION AND VALIDATION

The DSM2 model results of flow at Delta locations were used to calculate OMR flow as one input to the ANN model. DSM2-simulated turbidity at seven locations of interest from the twelve scenarios was used as training targets. During the training process, the model development dataset is usually divided into training, validation and testing purposes. The training dataset is used to compute the gradient and determine the model parameters (weights and bias). The validation dataset is used to find minimum error point and prevent over training. An error is monitored on the validation dataset during training. The validation error normally decreases during the initial phase of training, as does the training set error. However, when the network begins to over-fit the data, the error on the validation set typically begins to rise. When the validation error increases for a number of iterations, the training is stopped, and the parameters at the minimum validation error are returned. The test dataset is not used in the training (e.g., for stopping the network) and provides an independent evaluation on network performance.

In this work, the data was divided in the following manner: 60%, 20%, and 20% was used for training, validation and testing, respectively. The data points for training, validation and testing were randomly selected from the entire dataset for each training cycle.

# 3 RESULTS

## 3.1 DSM2 SIMULATED TURBIDITY AT TARGET LOCATIONS

The DSM2 simulated turbidity time series at seven target locations for each of the twelve scenarios are presented below (Figure 3-1 through Figure 3-7). To ensure that the DSM2 outputs in this work were identical to those obtained by DWR, values were compared to those in Liu and Sandhu (2011) using identical inputs and output time periods. This information is presented in Appendix B for different locations in the Delta.

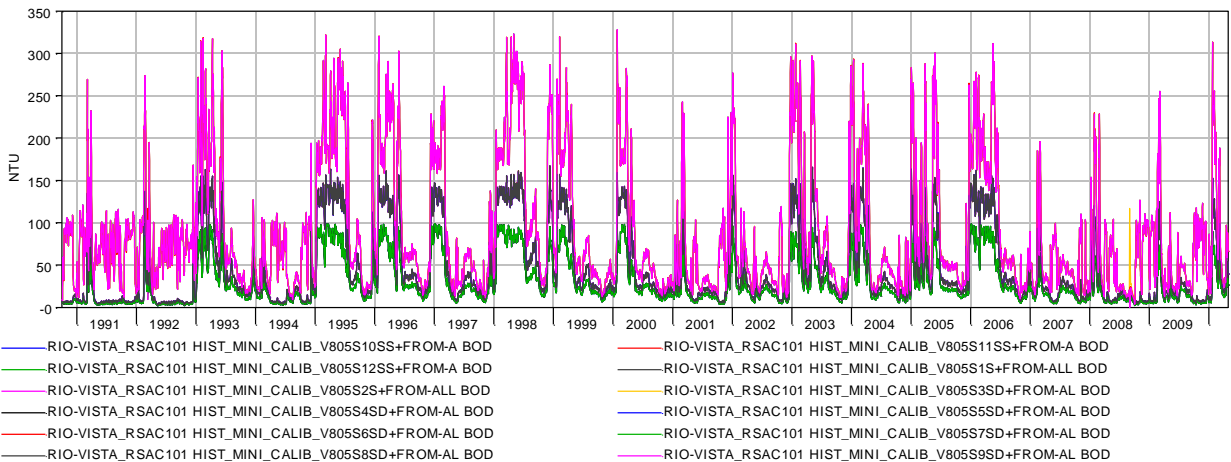


Figure 3-1 DSM2 simulated turbidity under twelve boundary conditions at Sacramento River at Rio Vista. Each line in this plot corresponds to a single boundary condition in Table 2-1.

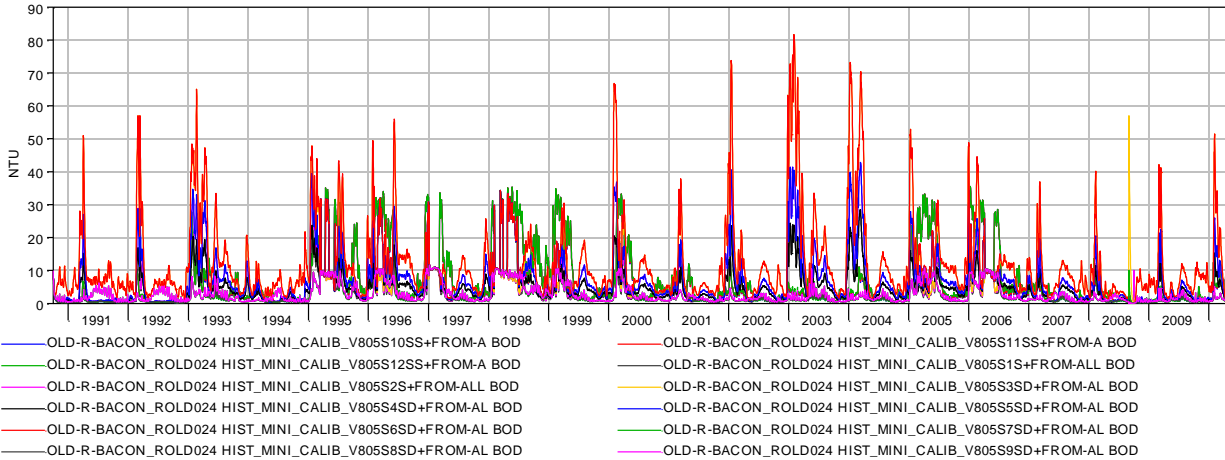


Figure 3-2 DSM2 simulated turbidity under twelve boundary conditions at Old River at Bacon Island.

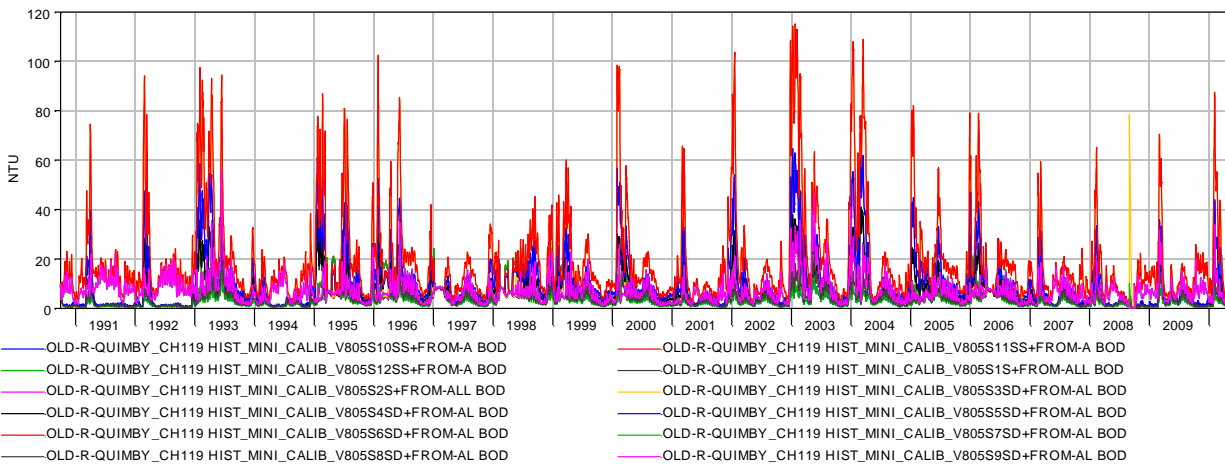


Figure 3-3 DSM2 simulated turbidity under twelve boundary conditions at Old River at Quimby Island.

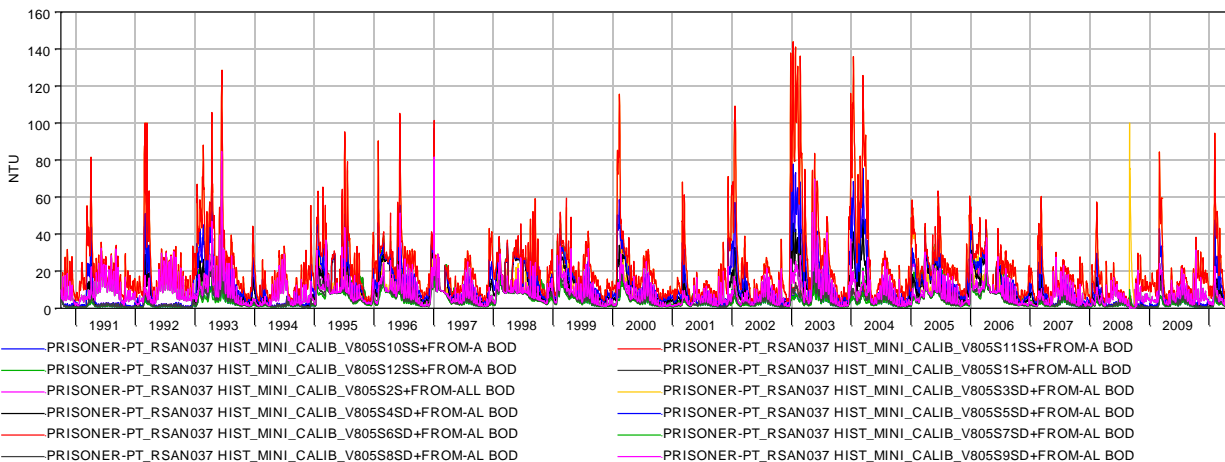


Figure 3-4 DSM2 simulated turbidity under twelve boundary conditions at San Joaquin River at Prisoner's Point.

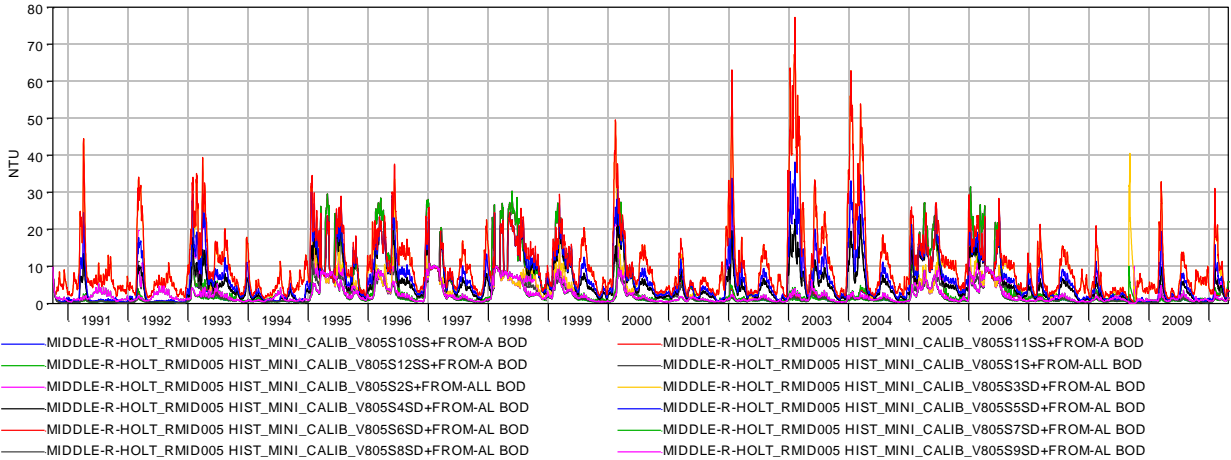


Figure 3-5 DSM2 simulated turbidity under twelve boundary conditions at Middle River at Holt.

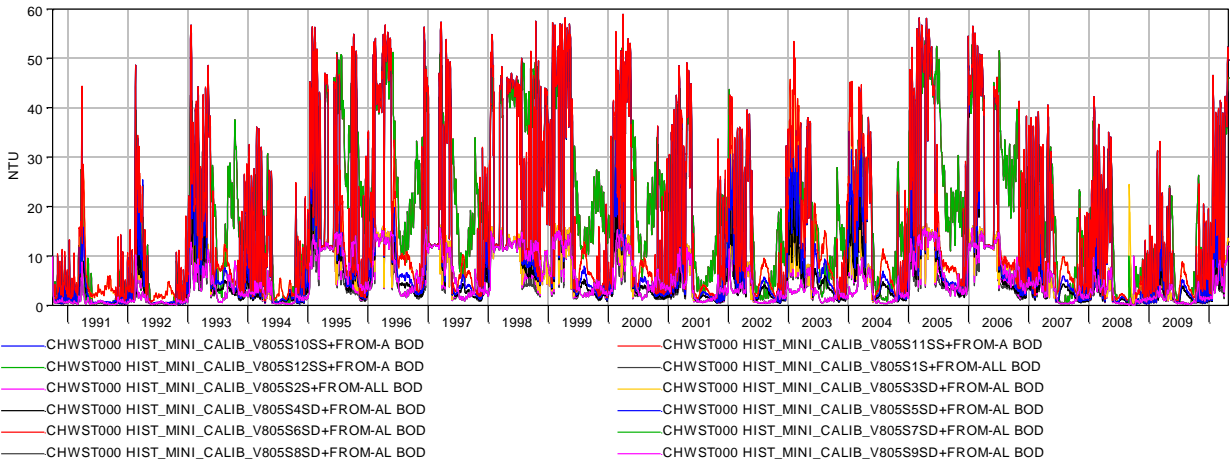


Figure 3-6 DSM2 simulated turbidity under twelve boundary conditions at Clifton Court Forebay.

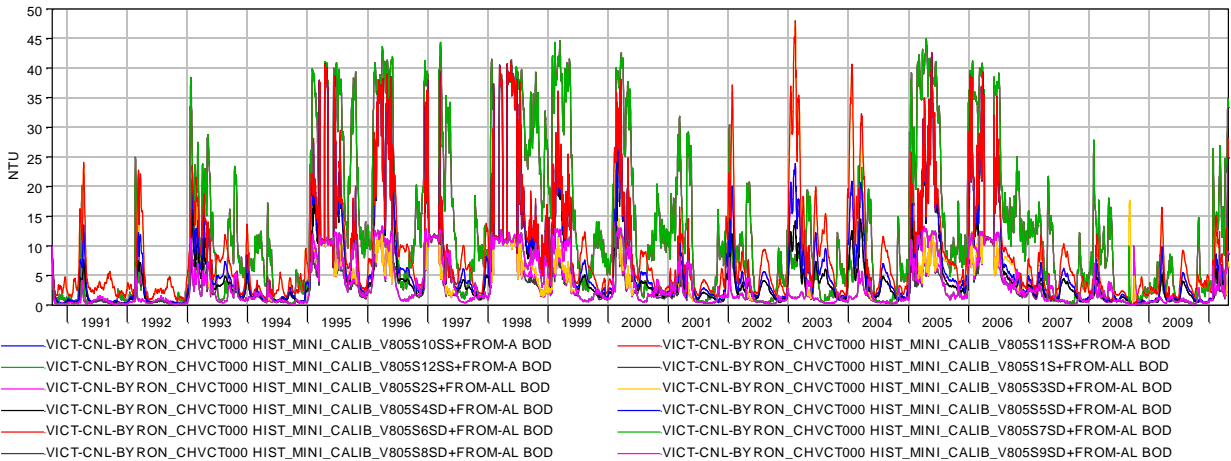


Figure 3-7 DSM2 simulated turbidity under twelve boundary conditions at Victoria Canal.

### 3.2 ANN TRAINING RESULTS

The ANN models for the seven target locations were trained for feed-forward networks using the back propagation method. The structure of the network (number of neurons and days of time lag) was determined through trial and error, by comparing training results with different network size and time of delay. An optimal size of 15 neurons and 4 days of time delay was found, when the correlation between ANN and DSM2 simulated values was the highest (Figure 3-8). A network size with 15 neurons was selected because it shows some improvement in predictions at selected locations (Middle River at Holt and Victoria Canal). There is also improvement in predictions from increasing of time delay from 2 days to 4 days. A 15-neuron model is considered appropriate for the current application, however, if computational efficiency is more important, a network size of 10 neurons may be used. The fit obtained by the NARX model using an open loop (i.e., using the actual DSM2 values from the output locations as well as the boundary locations as part of the training) is also shown and is consistently higher than that obtained from the feed-forward network, that is based only on values from boundary locations. For the trained feed-forward network, the quality of the fit for subsets of the data, i.e., the data used for training, validation, and testing, as well as all data, are shown in Figure 3-9. Training and validation data sets have a high value of correlation coefficient (R), with the independent test data set being only marginally lower. The comparison of the trained and fitted values and the error associated with the training are shown in time series form in Appendix C.

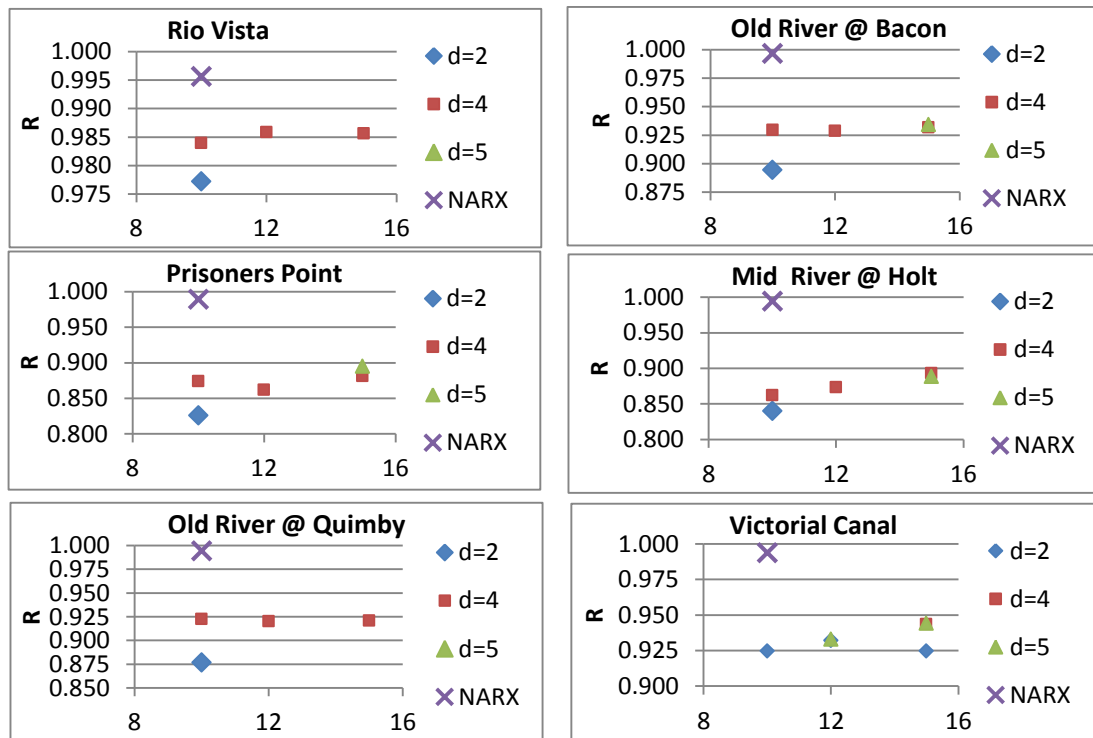


Figure 3-8. Correlation coefficient (R) between trained and target turbidity values for different sizes of the network, shown on the x-axis as the number of neurons, and using NARX open loop structure. d represents the days of delay in the input.

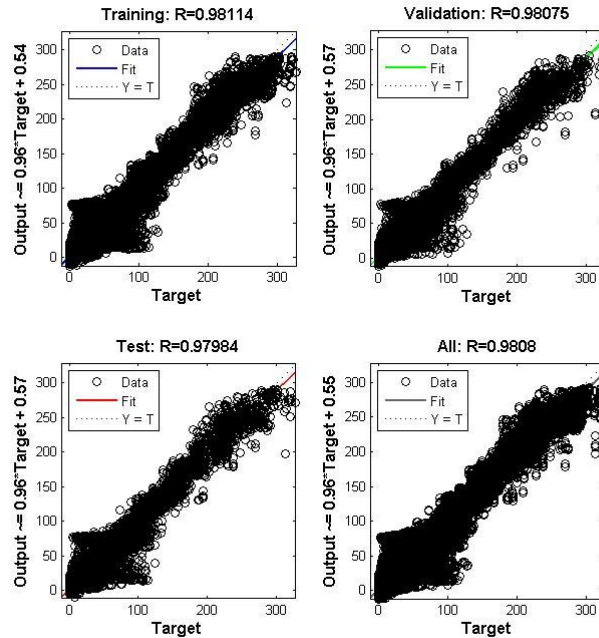


Figure 3-9. Correlation between trained and DSM2 simulated turbidity for the training, validation and test dataset for feed-forward network training.

The results of the training are presented as time-series of ANN-simulated turbidity compared to DSM2-simulated turbidity at target locations and correlation between ANN and DSM2 simulated daily and monthly turbidity (Figure 3-10 to Figure 3-23). The seven locations can be trained as one model (with one single measure of error for seven output variables) or as seven separate models (with a separate measure of error for each output variable). For brevity, the results for one single model training for one representative scenario, Scenario 5 in Table 2-1, is shown for the time series plots presented here. The scatter plots comparing ANN and DSM2 results, however, show values for 12 scenarios evaluated. Results for ANN training for all the twelve scenario boundary conditions are shown in Appendix D. Comparison of the use of a single model for all seven output stations against the use of seven separate ANNs is presented in a later section.

The single ANN model is generally able to capture temporal variations, in turbidity particularly during winter months of December–February. The correlation between ANN and DSM2 simulated turbidity is fairly good at different locations for daily values ( $R^2 = 0.75 - 0.97$ ) and improved for monthly values ( $R^2 = 0.84 - 0.996$ ) (Table 3-1). The evaluation for both time steps (daily and monthly) was due to potential uses of this methodology for different planning purposes in the Delta: Operations planning will be mainly focused on daily estimates, however, longer-term water allocation planning through CALSIM will be focused on monthly estimates. Because the range of turbidities found at Rio Vista are the broadest of all output stations considered here, the fit was significantly better for this station than other stations. More importantly, the better fit

could be due to that impulse-response is less complex at Rio Vista, as Rio Vista is mainly influenced by the North Delta boundary.

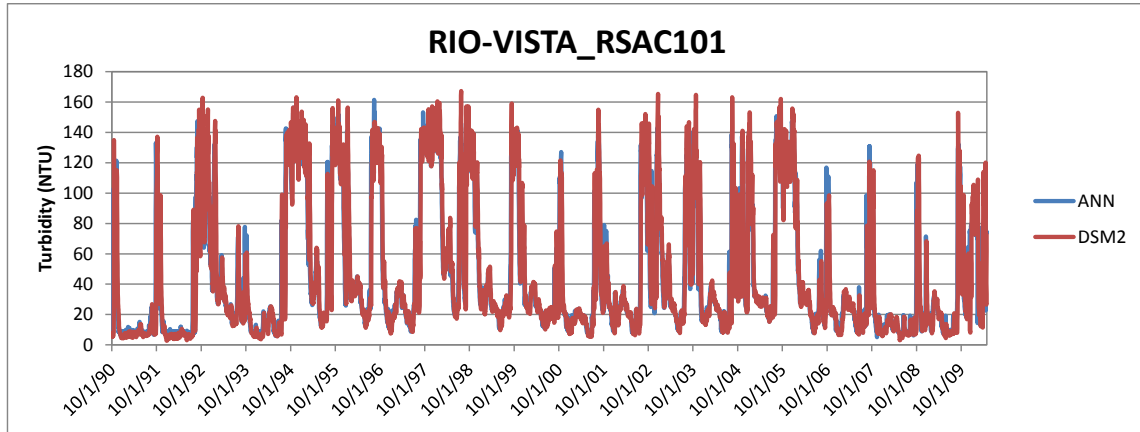


Figure 3-10 DSM2 and ANN simulated time-series turbidity at Sacramento River at Rio Vista (scenario 5).

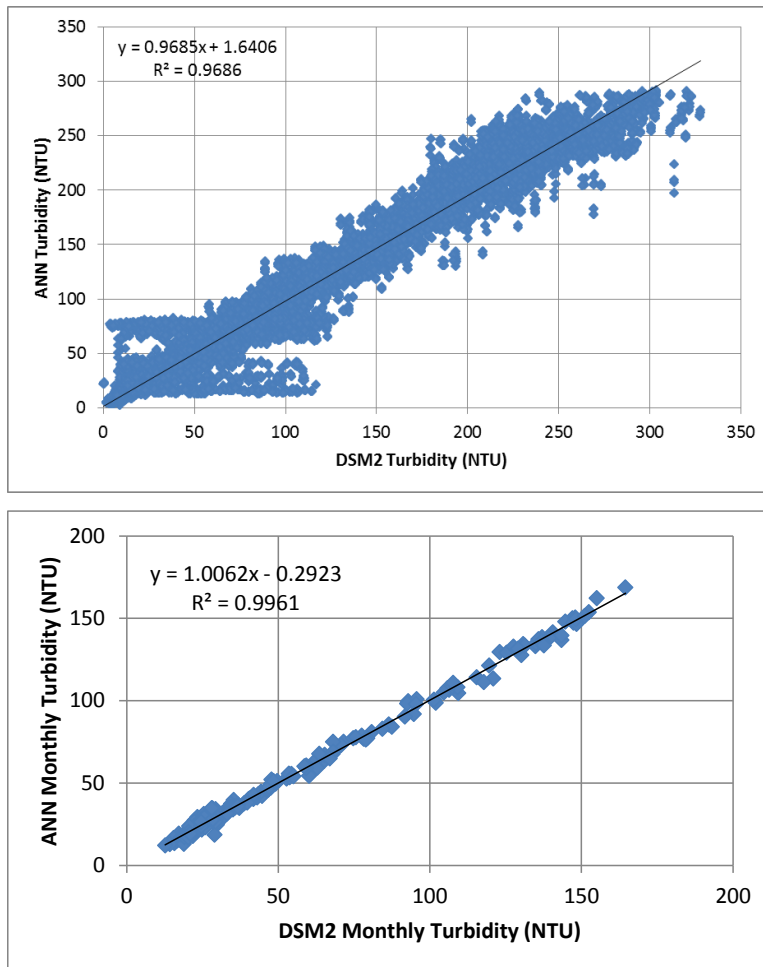


Figure 3-11 DSM2 and ANN simulated daily and monthly turbidity at Sacramento River at Rio Vista (all data).

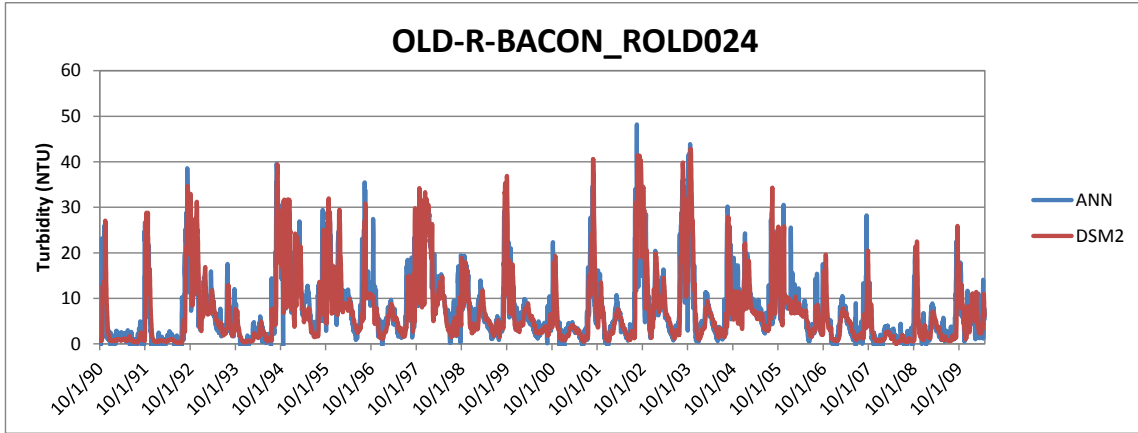


Figure 3-12 DSM2 and ANN simulated turbidity at Old River at Bacon Island (scenario 5).

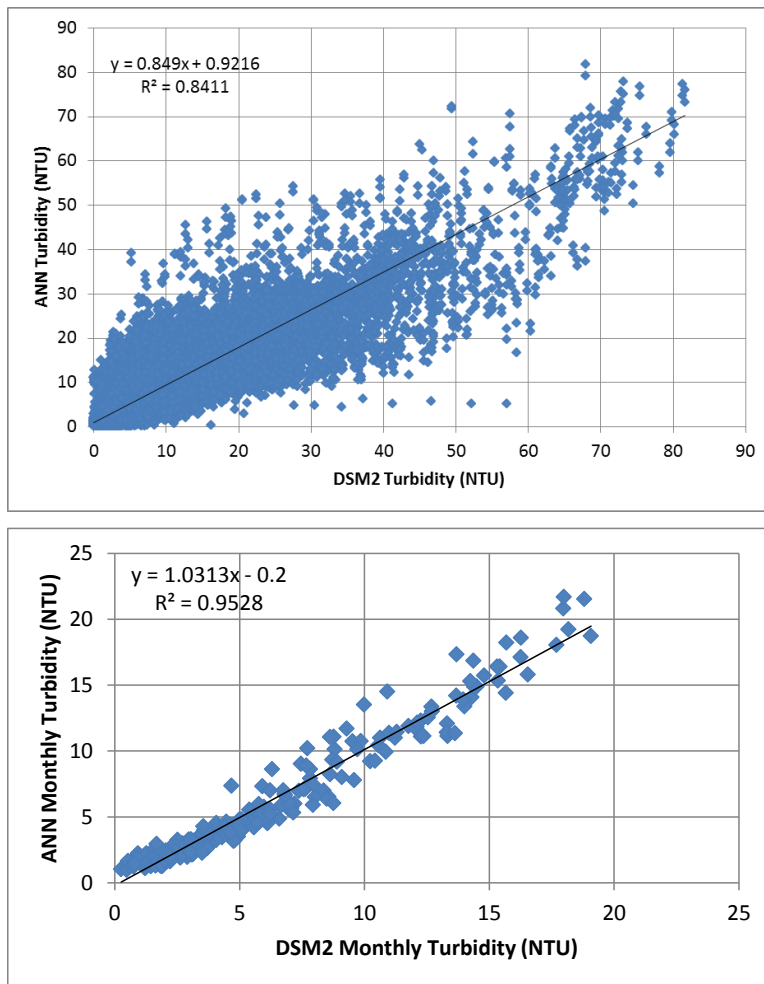


Figure 3-13 DSM2 and ANN simulated daily and monthly turbidity at Old River at Bacon Island (all data).

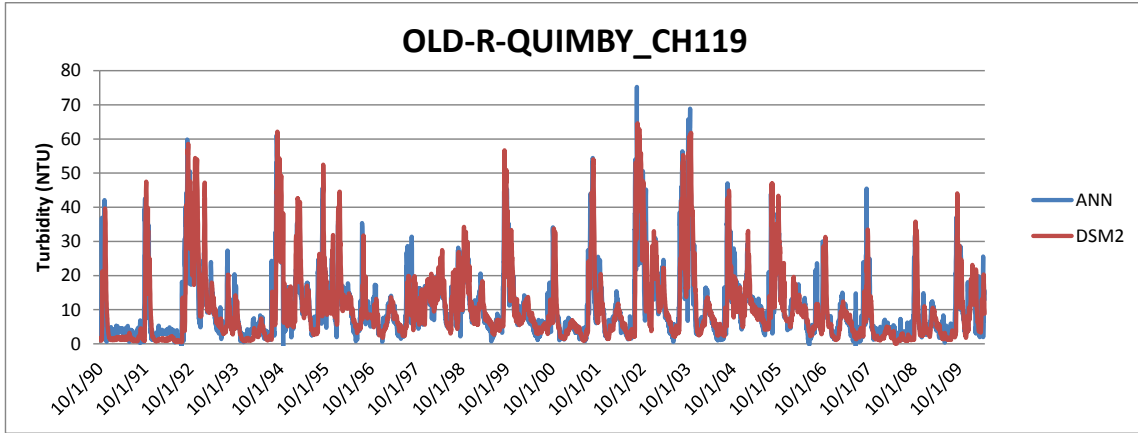


Figure 3-14 DSM2 and ANN simulated time-series turbidity at Old River at Quimby Island (scenario 5).

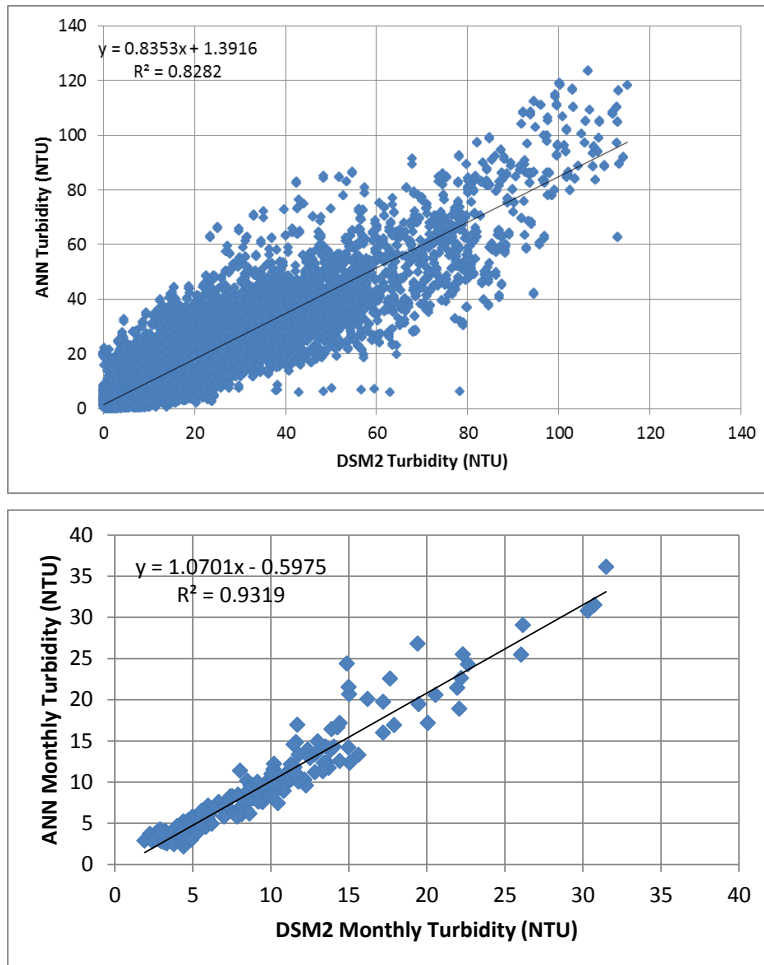


Figure 3-15 DSM2 and ANN simulated daily and monthly turbidity at Old River at Quimby Island (all data).

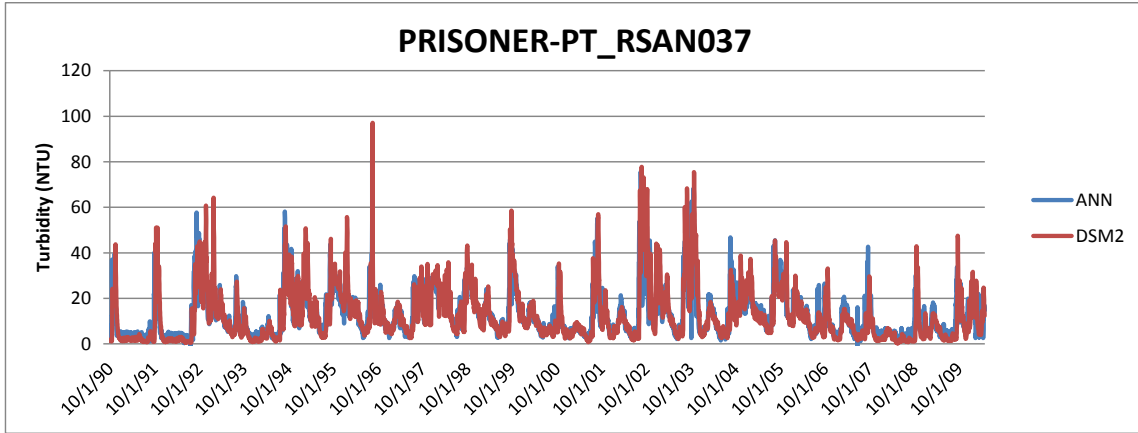


Figure 3-16 DSM2 and ANN simulated turbidity at San Joaquin River at Prisoner's Point (scenario 5).

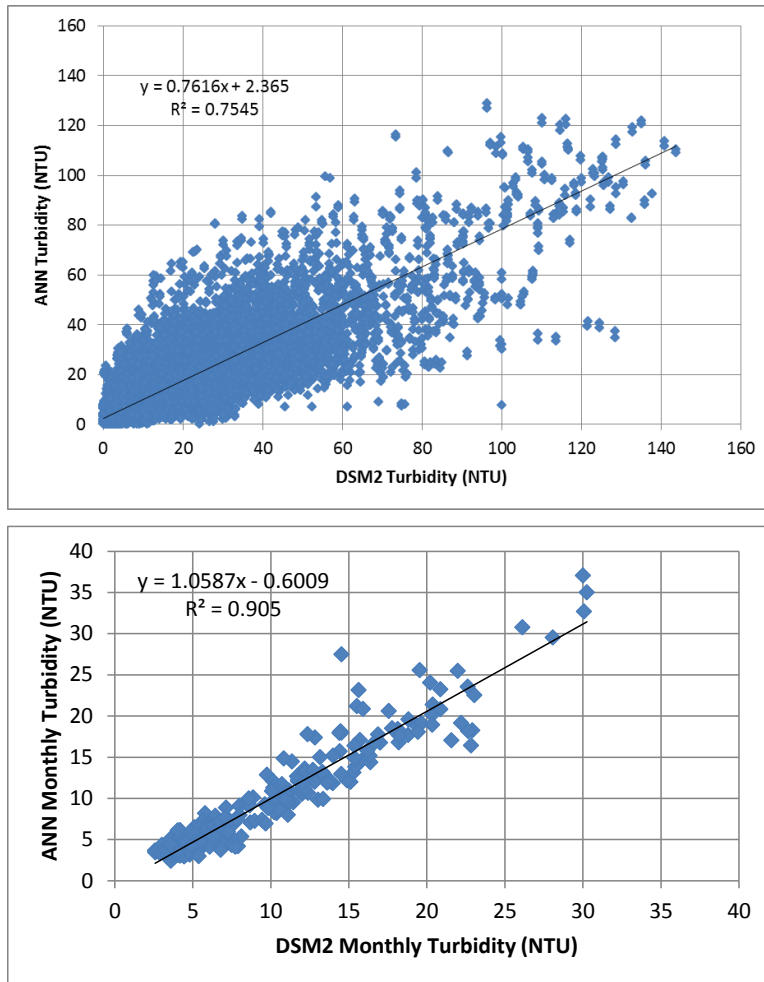


Figure 3-17 DSM2 and ANN simulated daily and monthly turbidity at San Joaquin River at Prisoner's Point (all data).

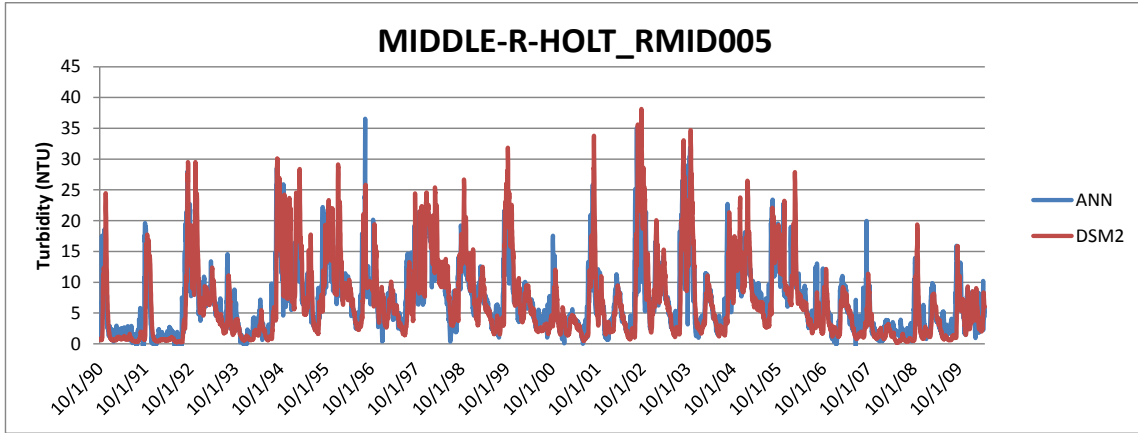


Figure 3-18 DSM2 and ANN simulated turbidity at Middle River at Holt (scenario 5).

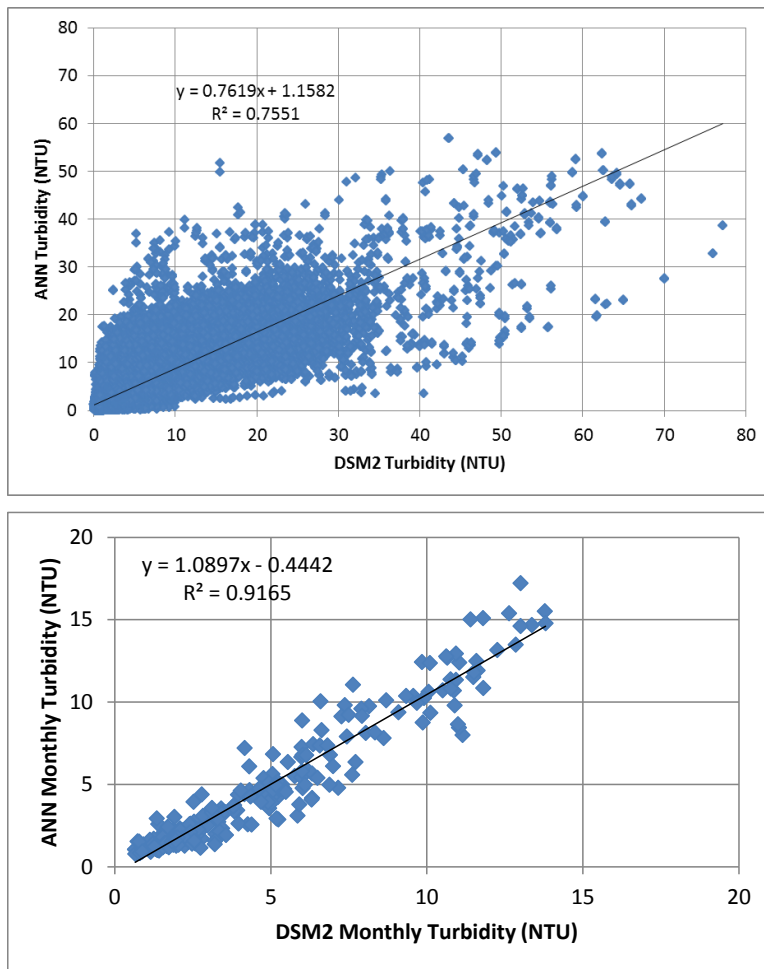


Figure 3-19 DSM2 and ANN simulated daily and monthly turbidity at Middle River at Holt (all data).

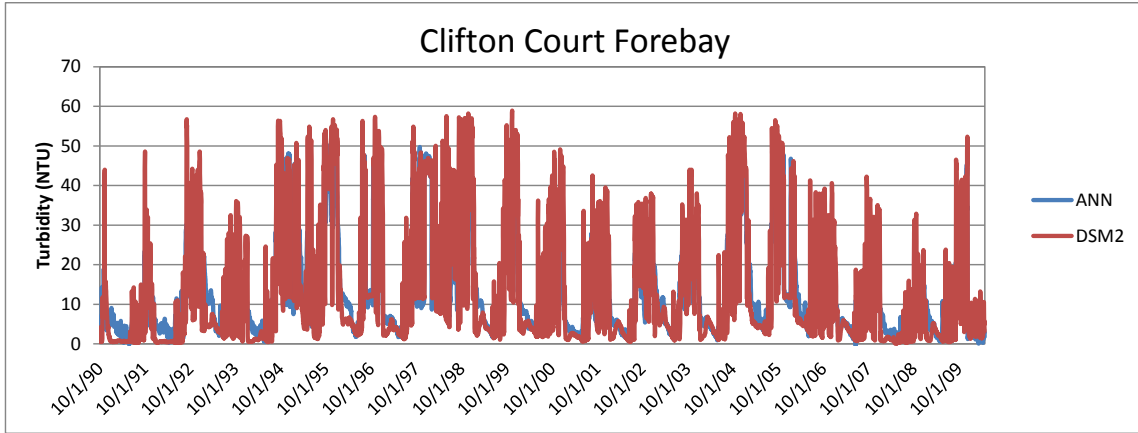


Figure 3-20 DSM2 and ANN simulated turbidity at Clifton Court Forebay Entrance (scenario 5).

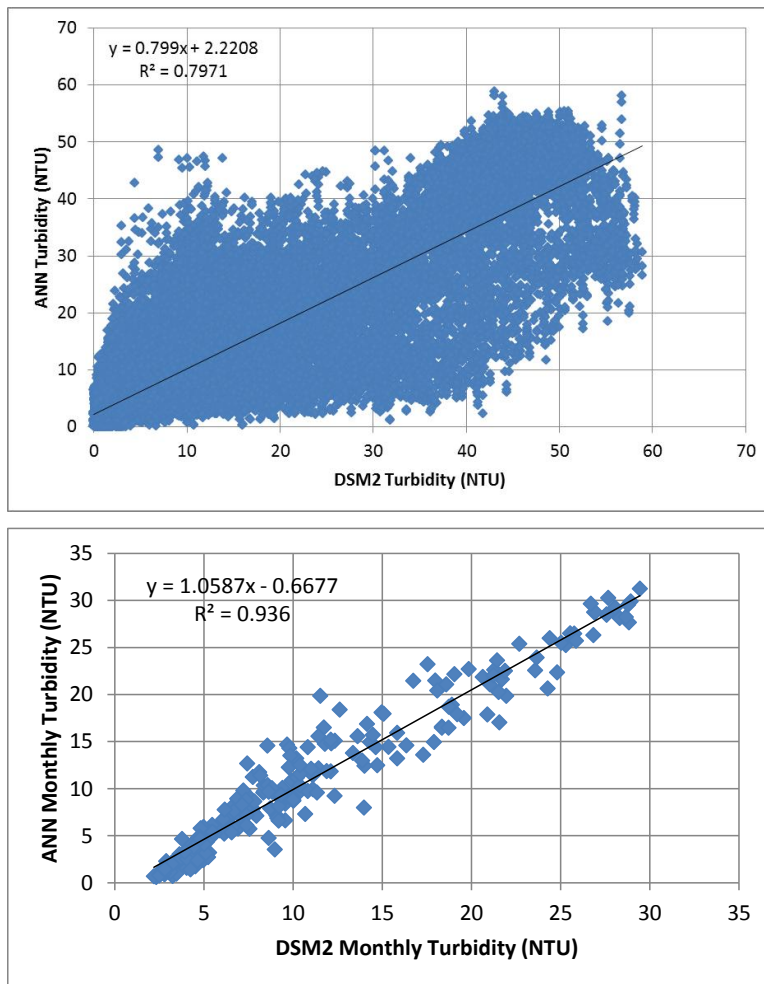


Figure 3-21 DSM2 and ANN simulated daily and monthly turbidity at Clifton Court Forebay (all data).

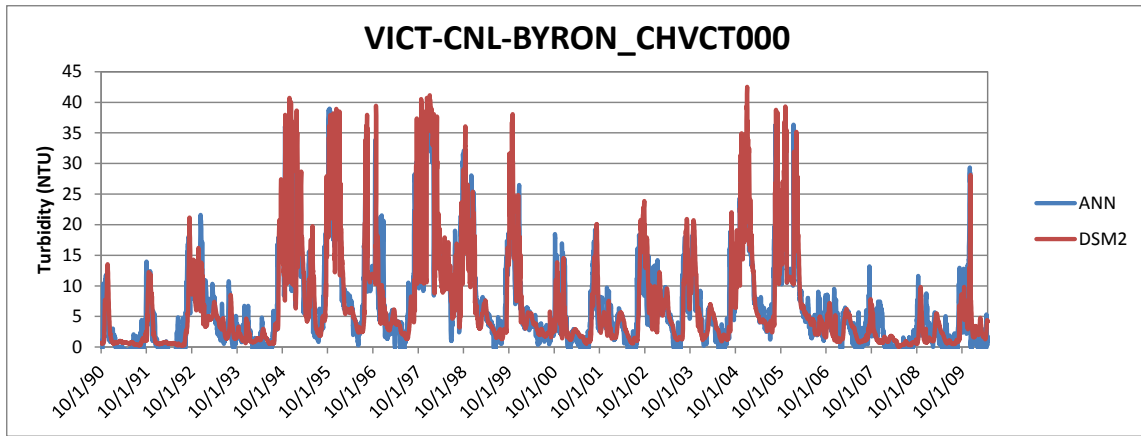


Figure 3-22 DSM2 and ANN simulated turbidity at Victoria Canal (scenario 5).

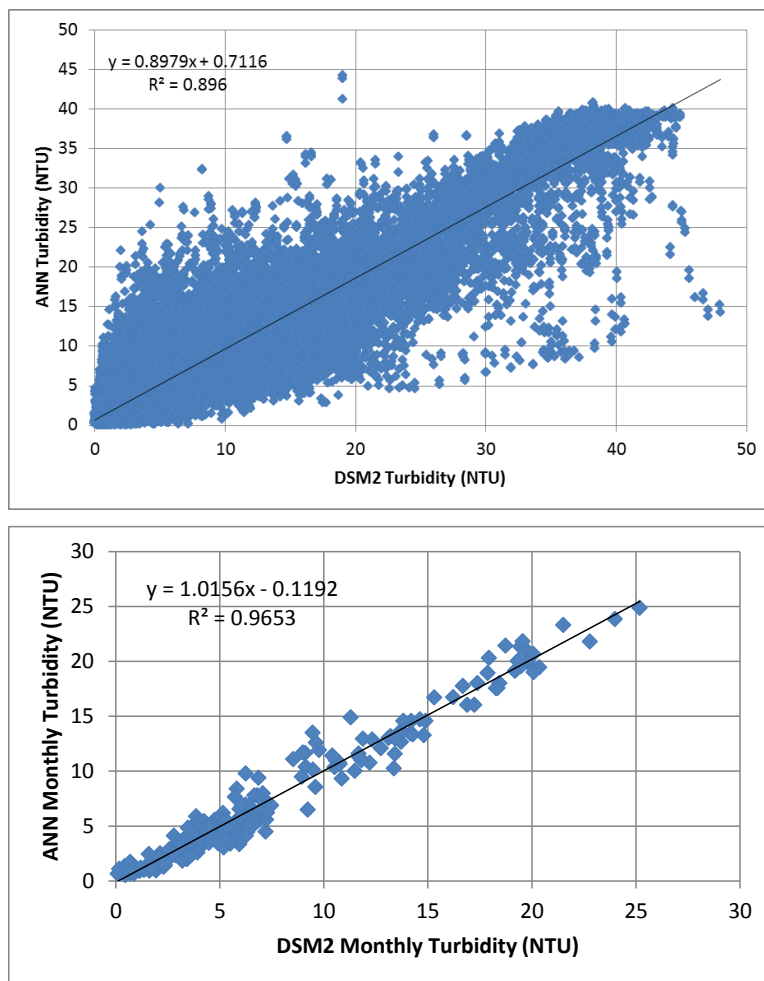


Figure 3-23 DSM2 and ANN simulated turbidity at Victoria Canal (all data).

**Table 3-1**  
**Comparison of ANN and DSM2 Simulated Turbidity at**  
**Delta Locations ANN Turbidity (ntu) =  $\Phi 1 + \Phi 2 \cdot \text{DSM2 turbidity (ntu)}$**   
**(R = correlation coefficient; SE = Standard Error)**

Location	Daily				Monthly			
	$\Phi 2$	$\Phi 1$	R <sup>2</sup>	SE	$\Phi 2$	$\Phi 1$	R <sup>2</sup>	SE
Clifton Court Forebay Entrance	0.799	2.2208	0.797	5.548	1.0587	-0.667	0.936	2.090
Middle River @ Holt	0.7619	1.1582	0.755	2.693	1.0897	-0.444	0.917	1.166
Old River @ Bacon Island	0.849	0.9216	0.841	2.885	1.0313	-0.200	0.953	1.082
Old River @ Quimby Island	0.8353	1.3916	0.828	4.247	1.0701	-0.5975	0.932	1.637
San Joaquin River @ Prisoner's Point	0.7616	2.365	0.755	5.535	1.0587	-0.6009	0.905	2.107
Sacramento River @ Rio Vista	0.9685	1.6406	0.969	10.080	1.0062	-0.2923	0.996	2.598
Victoria Canal	0.8979	0.7116	0.896	2.417	1.0156	-0.1192	0.965	1.118

### 3.3 TRAINING WITH TIDAL EFFECTS

The time-series plots of ANN training results shown above at several locations (e.g., Clifton Court Forebay, Old River at Bacon) suggested that some tidal effects may not be accounted for by the ANN training, although they are part of the DSM2 model (an example is shown in Figure 3-24). This is due to tides not being part of the ANN model inputs in the results shown thus far. To account for tidal effects on Delta turbidity and subsequently impacts of tides on the ANN training, a tidal input was added to the ANN model. A tidal input was added by introducing a DSM2-simulated OMR flow, an input which retains the information on tidal variation. The results of using this alternative OMR flow as ANN model input are presented below (Figure 3-25 to Figure 3-38). The results show no significant improvement in model agreement with DSM2 simulated turbidities. The correlation between ANN simulated turbidity with tidal effect and the DSM2 generated turbidity is broadly similar at different locations for daily (R<sup>2</sup> = 0.69 – 0.94) and monthly (R<sup>2</sup> = 0.89 – 0.99) results (Table 3-2).

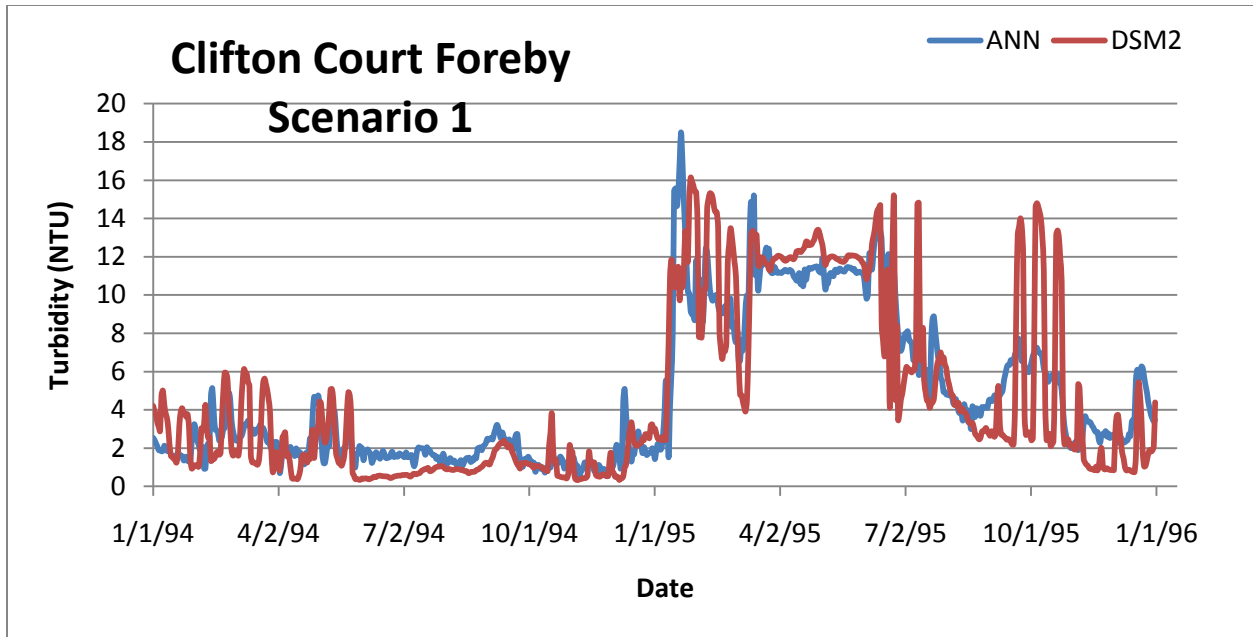


Figure 3-24 DSM2 and ANN simulated (with tidal effect) time-series turbidity.

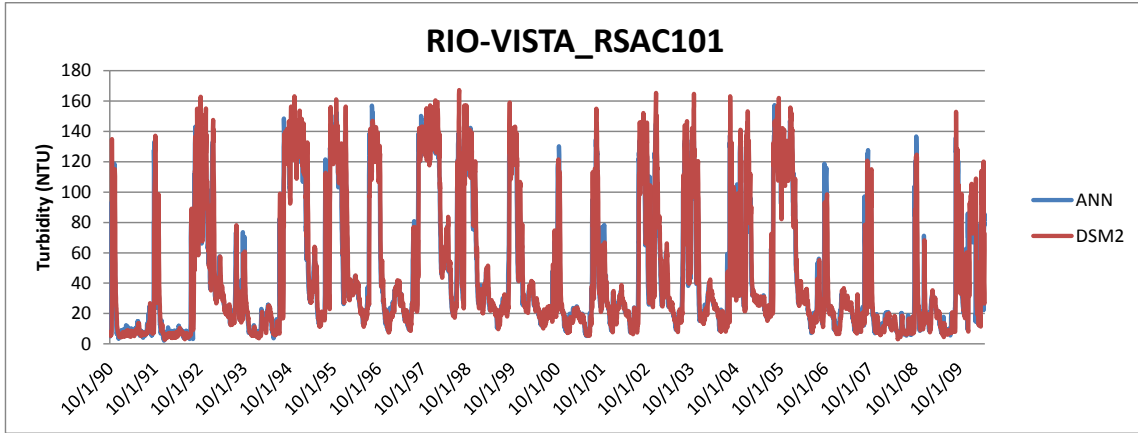


Figure 3-25 DSM2 and ANN simulated (with tidal effect) time-series turbidity at Sacramento River at Rio Vista (scenario 5).

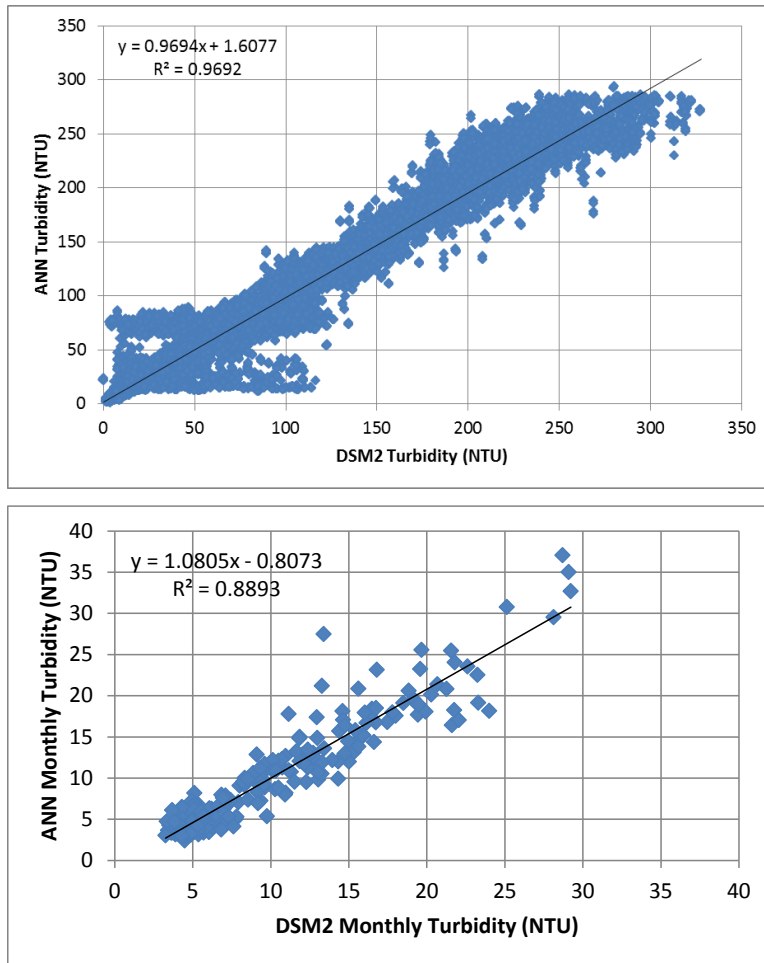


Figure 3-26 DSM2 and ANN simulated (with tidal effect) daily and monthly turbidity at Sacramento River at Rio Vista (all data).

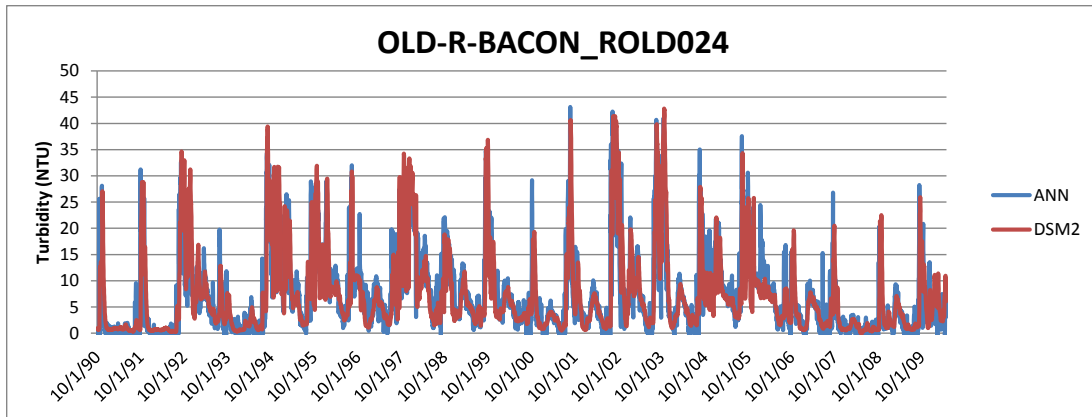


Figure 3-27 DSM2 and ANN simulated (with tidal effect) turbidity at Old River at Bacon Island (scenario 5).

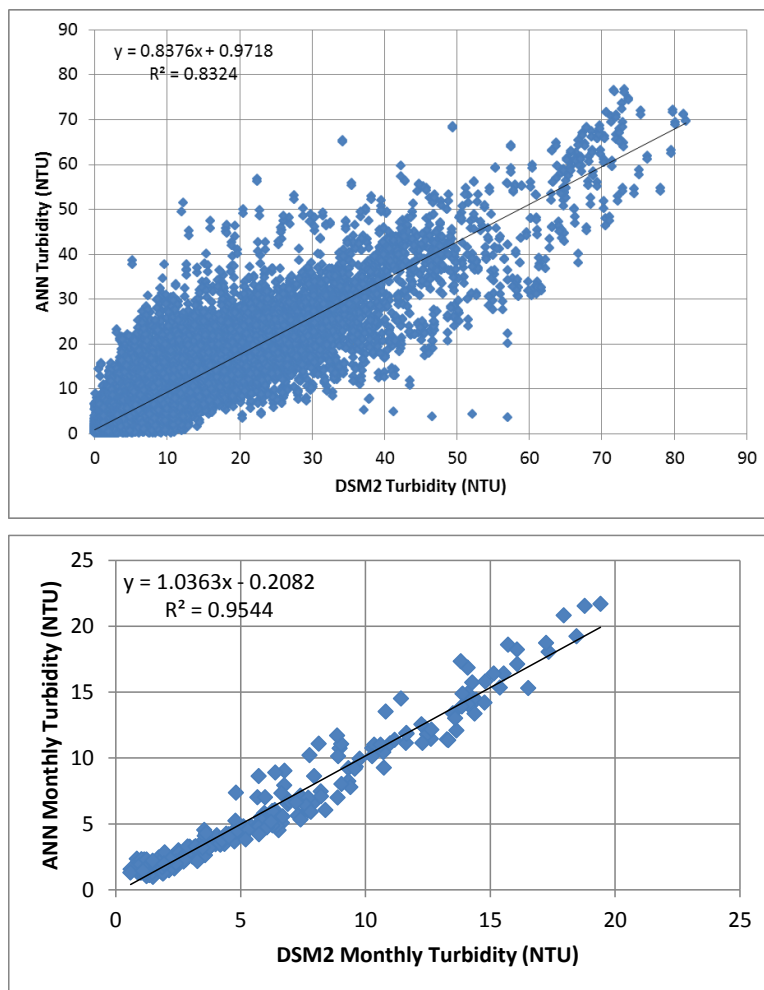


Figure 3-28 DSM2 and ANN simulated (with tidal effect) daily and monthly turbidity at Old River at Bacon Island (all data).

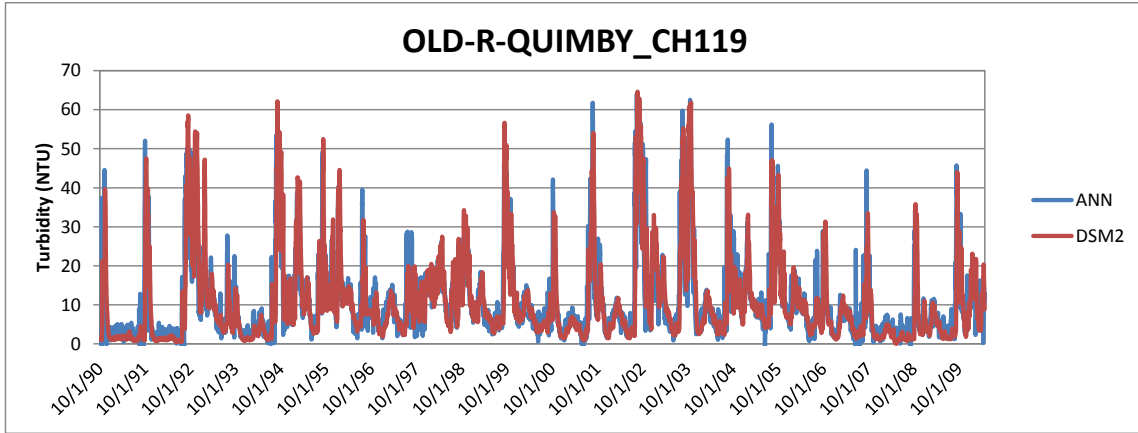


Figure 3-29 DSM2 and ANN simulated (with tidal effect) time-series turbidity at Old River at Quimby Island (scenario 5).

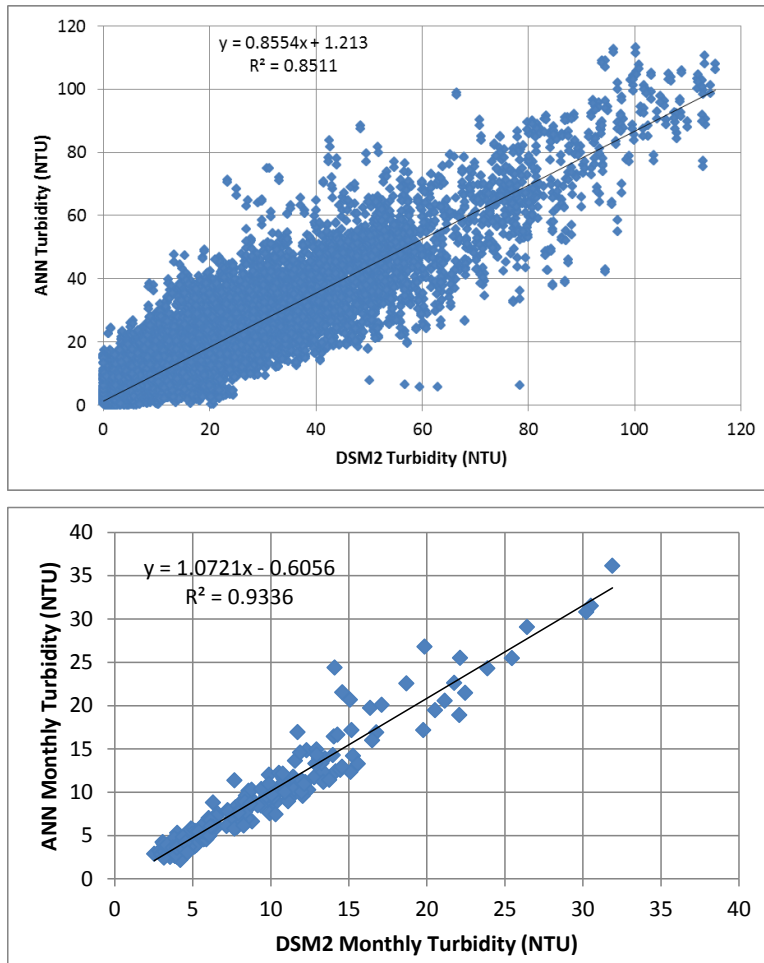


Figure 3-30 DSM2 and ANN simulated (with tidal effect) daily and monthly turbidity at Old River at Quimby Island (all data).

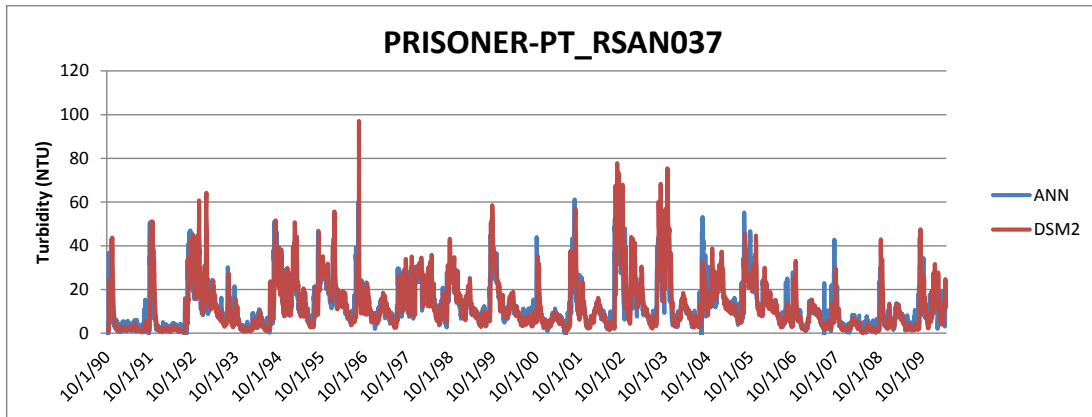


Figure 3-31 DSM2 and ANN simulated (with tidal effect) turbidity at San Joaquin River at Prisoner's Point (scenario 5).

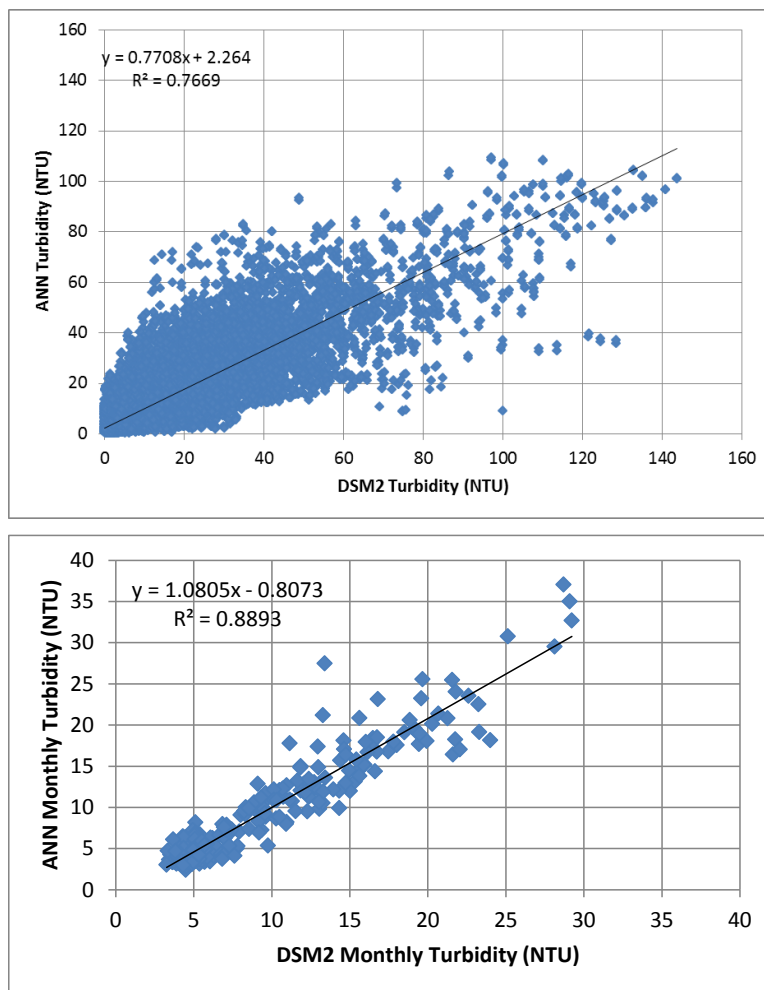


Figure 3-32 DSM2 and ANN simulated (with tidal effect) daily and monthly turbidity at San Joaquin River at Prisoner's Point (all data).

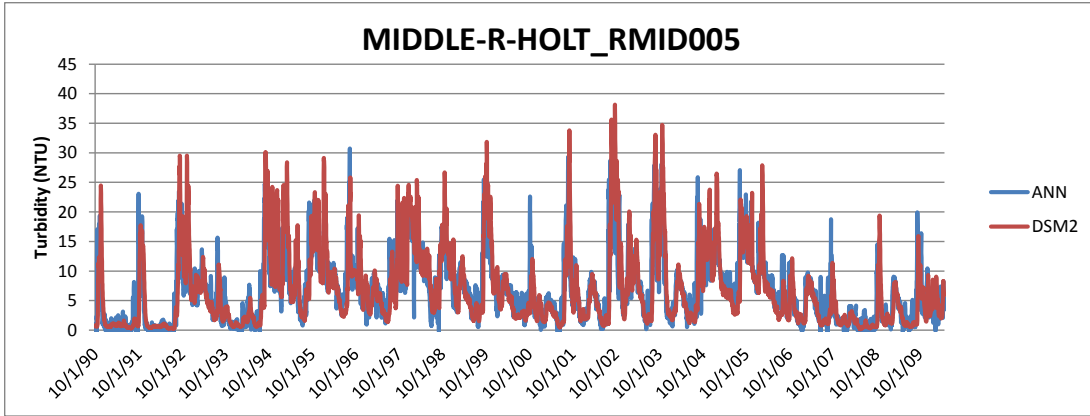


Figure 3-33 DSM2 and ANN simulated (with tidal effect) turbidity at Middle River at Holt (scenario 5).

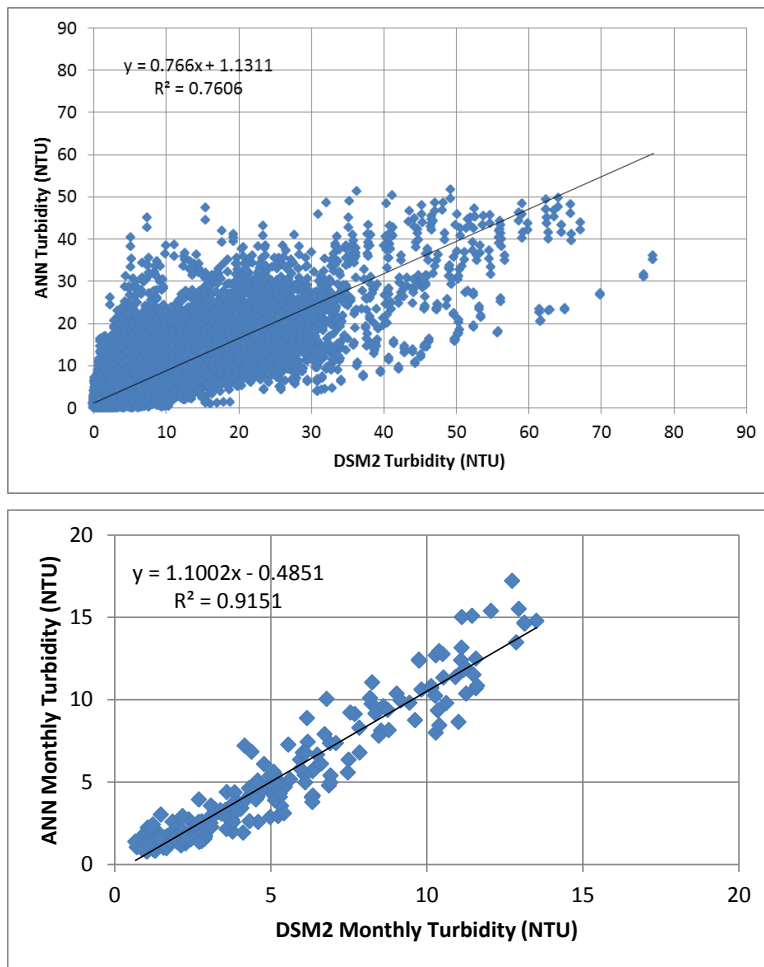


Figure 3-34 DSM2 and ANN simulated (with tidal effect) daily and monthly turbidity at Middle River at Holt (all data).

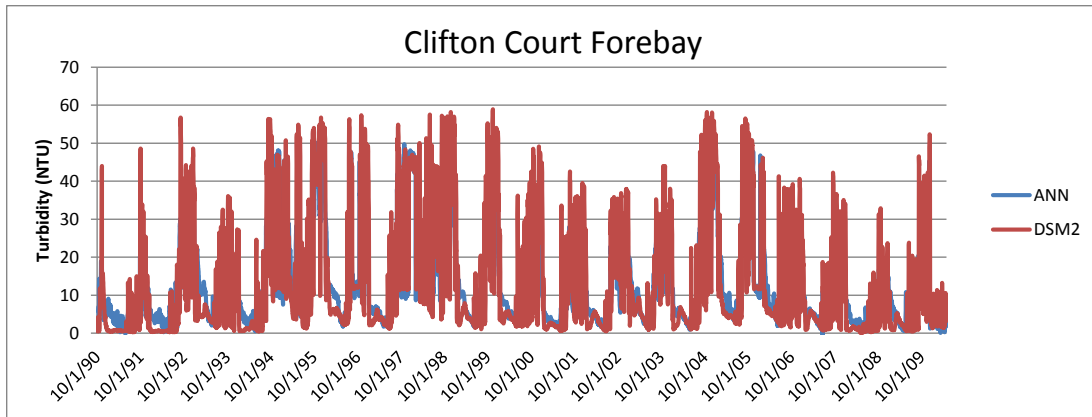


Figure 3-35 DSM2 and ANN simulated (with tidal effect) turbidity at Clifton Court Forebay Entrance (scenario 5).

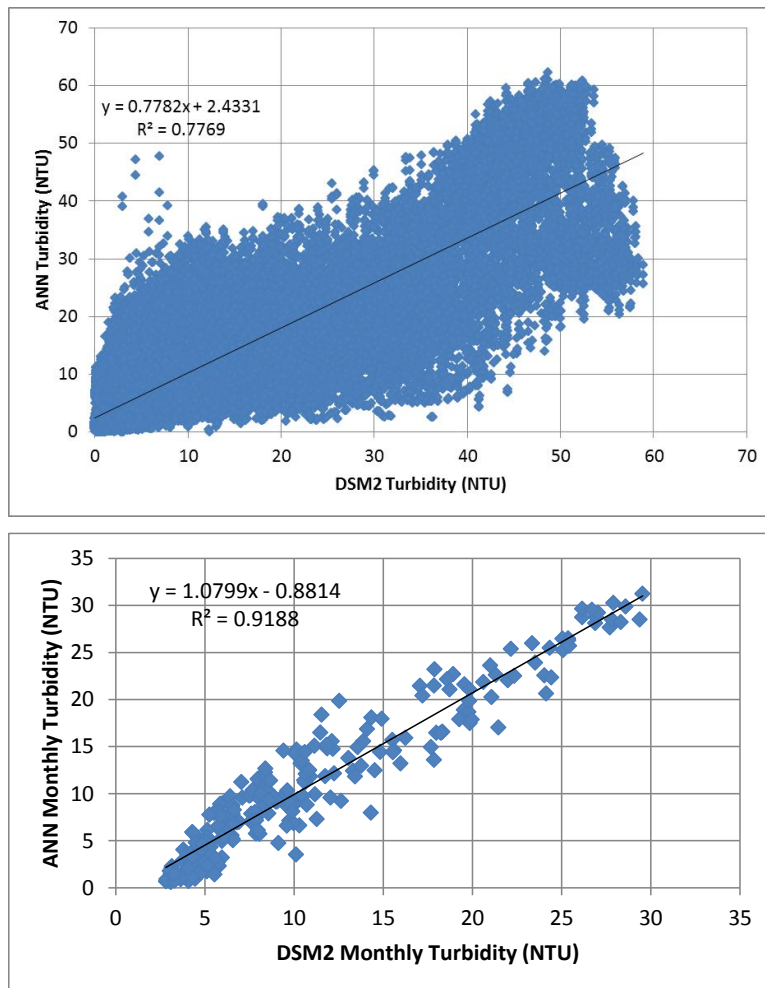


Figure 3-36 DSM2 and ANN simulated (with tidal effect) daily and monthly turbidity at Clifton Court Forebay (all data).

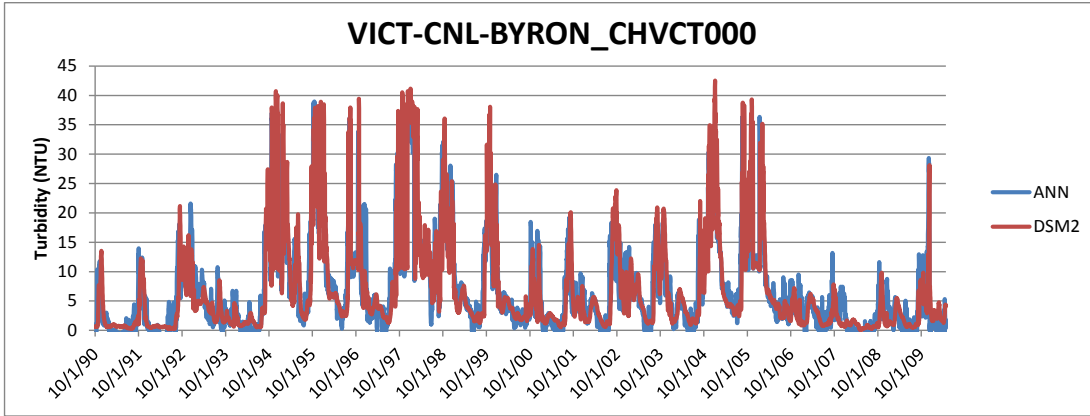


Figure 3-37 DSM2 and ANN simulated (with tidal effect) turbidity at Victoria Canal (scenario 5).

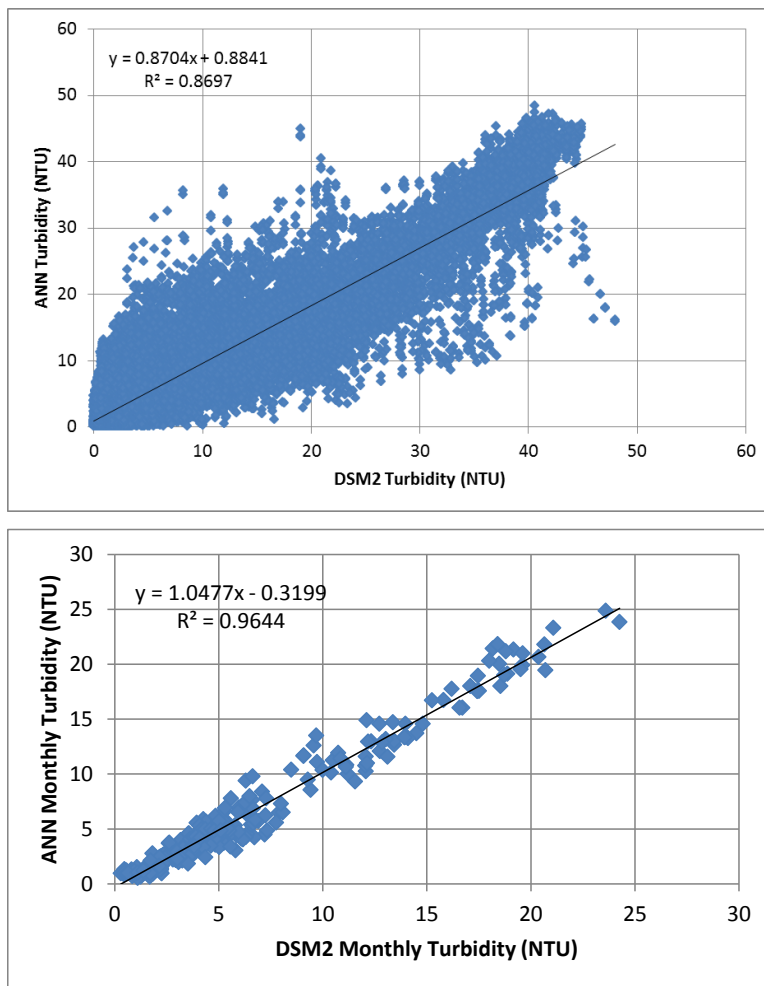


Figure 3-38 DSM2 and ANN simulated (with tidal effect) daily and monthly turbidity at Victoria Canal (all data).

**Table 3-2**  
**Comparison of ANN and DSM2 Simulated Turbidity at Delta Locations**  
**with Tidal Effects ANN Turbidity (ntu) =  $\Phi 1 + \Phi 2 * \text{DSM2 turbidity (ntu)}$**   
**(R = correlation coefficient; SE = Standard Error)**

Location	Daily				Monthly			
	$\Phi 2$	$\Phi 1$	R <sup>2</sup>	SE	$\Phi 2$	$\Phi 1$	R <sup>2</sup>	SE
Clifton Court Forebay Entrance	0.7782	2.4331	0.777	5.836	1.0799	-0.8814	0.919	2.373
Middle River @ Holt	0.766	1.1311	0.761	2.666	1.1002	-0.4851	0.915	1.184
Old River @ Bacon Island	0.8376	0.9718	0.832	2.987	1.0363	-0.2082	0.954	1.068
Old River @ Quimby Island	0.8554	1.213	0.851	3.931	1.0721	-0.6056	0.934	1.620
San Joaquin River @ Prisoner's Point	0.7708	2.264	0.767	5.398	1.0805	-0.8073	0.889	2.291
Sacramento River @ Rio Vista	0.9694	1.6077	0.969	9.989	1.0064	-0.3208	0.996	2.639
Victoria Canal	0.8704	0.8841	0.870	2.813	1.0477	-0.3199	0.964	1.161

### 3.4 EVALUATION OF SINGLE ANN MODEL VERSUS SEVEN SEPARATE MODELS

Results for training as separate models for each individual output location were compared to the single model training (Table 3-3). When training as separate models, the measure of error of each variable was minimized separately, therefore should result in better model performance. The comparison shows a slight improvement over the single model training, however the improvement is not large enough to justify the use of multiple models.

**Table 3-3**  
**Comparison of Training Results Using One Single Model and**  
**Seven Separate Models ANN Turbidity (ntu) =  $\Phi 1 + \Phi 2 * \text{DSM2 turbidity (ntu)}$**   
**(R = correlation coefficient; SE = Standard Error)**

Location	One Model				Seven Models			
	$\Phi 2$	$\Phi 1$	R <sup>2</sup>	SE	$\Phi 2$	$\Phi 1$	R <sup>2</sup>	SE
Clifton Court Forebay Entrance	0.799	2.2208	0.797	5.548	0.8288	1.8836	0.828	5.079
Middle River @ Holt	0.7619	1.1582	0.755	2.693	0.8132	0.9037	0.808	2.295
Old River @ Bacon Island	0.849	0.9216	0.841	2.885	0.8618	0.8277	0.861	2.646
Old River @ Quimby Island	0.8353	1.3916	0.828	4.247	0.8727	1.0581	0.871	3.616
San Joaquin River @ Prisoner's Point	0.7616	2.365	0.755	5.535	0.7599	2.3895	0.758	5.495
Sacramento River @ Rio Vista	0.9685	1.6406	0.969	10.080	0.9717	1.5179	0.973	9.424
Victoria Canal	0.8979	0.7116	0.896	2.417	0.9242	0.5461	0.925	1.914

### 3.5 EVALUATION OF ALTERNATIVE NETWORK STRUCTURE

An alternative network structure, the nonlinear autoregressive network with exogenous inputs (NARX) network was explored as alternative structure for ANN training.

The results suggested notably increased correlation between ANN simulated and DSM2 turbidities by using the NARX open loop structure (Table 3-4, and representative location in Figure 3-39), where the inputs include boundary values and DSM2 generated values at output locations. A NARX trained in an open loop mode can be converted to closed loop NARX, where the ANN-predicted values from the preceding time-steps are used as input. The results suggest that when the network is converted to a closed loop, the predictions have no improvement over the feed-forward network (Table 3-4). However, the fact that the open loop network provides very high quality fits offers the promise that if there is information available at output locations from preceding time-steps, such as through the collection of real-time data embarked upon by the DWR since 2009, an ANN could be trained to provide higher quality predictions over short time frames.

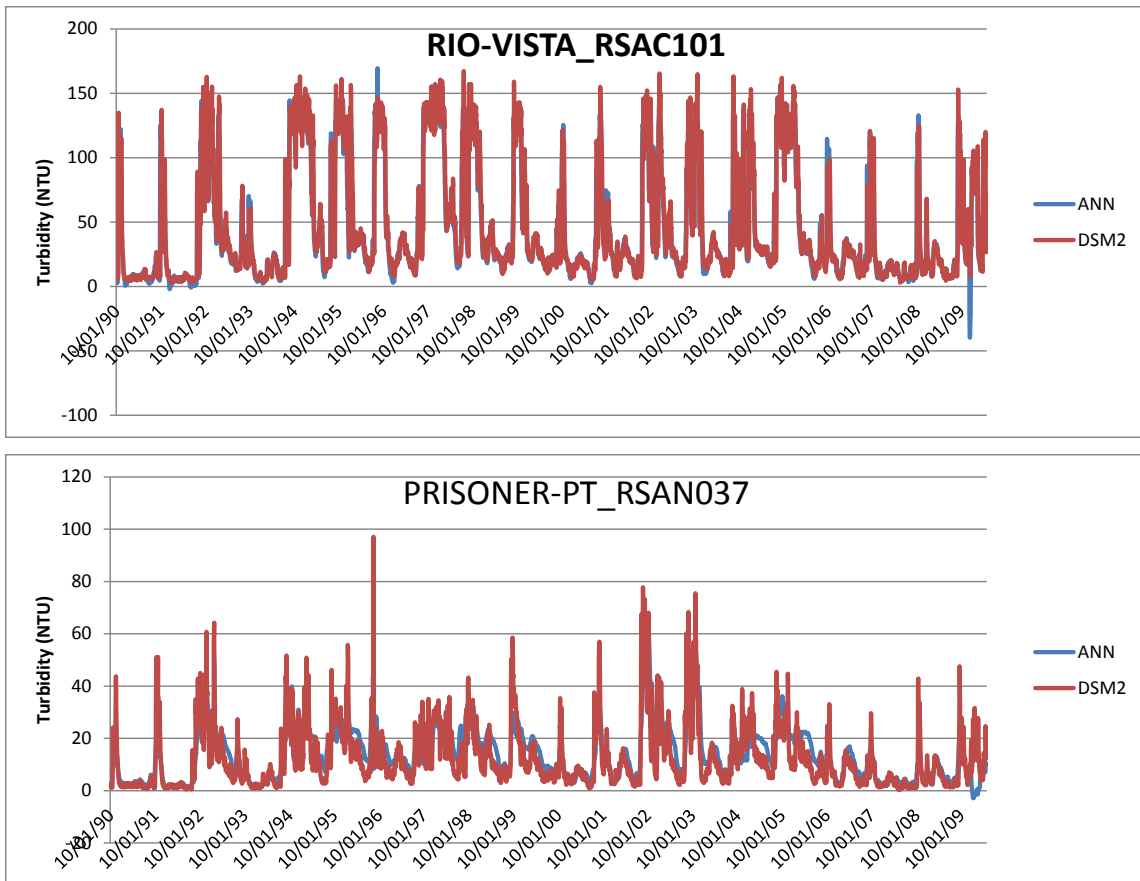


Figure 3-39 Example of ANN developed using the NARX structure. DSM2 and ANN simulated turbidity values are shown for Prisoner Point (scenario 5).

**Table 3-4**  
**Comparison of ANN and DSM2 Simulated Turbidity at Delta Locations**  
**using NARX Network ANN Turbidity (ntu) =  $\Phi 1 + \Phi 2 * \text{DSM2 turbidity (ntu)}$**   
**(R = correlation coefficient; SE = Standard Error)**

Location	Open				Closed			
	$\Phi 2$	$\Phi 1$	R <sup>2</sup>	SE	$\Phi 2$	$\Phi 1$	R <sup>2</sup>	SE
Middle River @ Holt	0.9776	0.1081	0.967	1.112	0.7773	2.010	0.404	6.030
Old River @ Bacon Island	0.9731	0.1634	0.957	1.673	0.6896	2.834	0.399	7.317
Old River @ Quimby Island	0.9650	0.2907	0.946	2.520	0.7418	2.314	0.605	7.040
San Joaquin River @ Prisoner's Point	0.9433	0.5523	0.910	3.470	0.7957	3.373	0.554	8.671
Sacramento River @ Rio Vista	0.9629	2.0420	0.936	14.506	0.9893	0.408	0.971	9.706
Victoria Canal	0.971	0.3196	0.988	1.383	0.6220	3.711	0.341	8.271

### 3.6 VALIDATION AGAINST HISTORICAL DATASET

The trained ANN network was validated using observed data obtained from CDEC for the period December 2009 through April 2010. The same dataset was used in the DSM2 turbidity calibration by Liu and Sandhu (2011). The ANN simulated turbidity was compared to observed values at seven target locations. The results suggest the ANN model is able to capture the dynamics of turbidity at various locations (Figure 3-40). In particular, the ANN was able to produce reasonable estimates at 5 of the 7 locations examined, the exceptions being Clifton Court and Middle River at Holt.

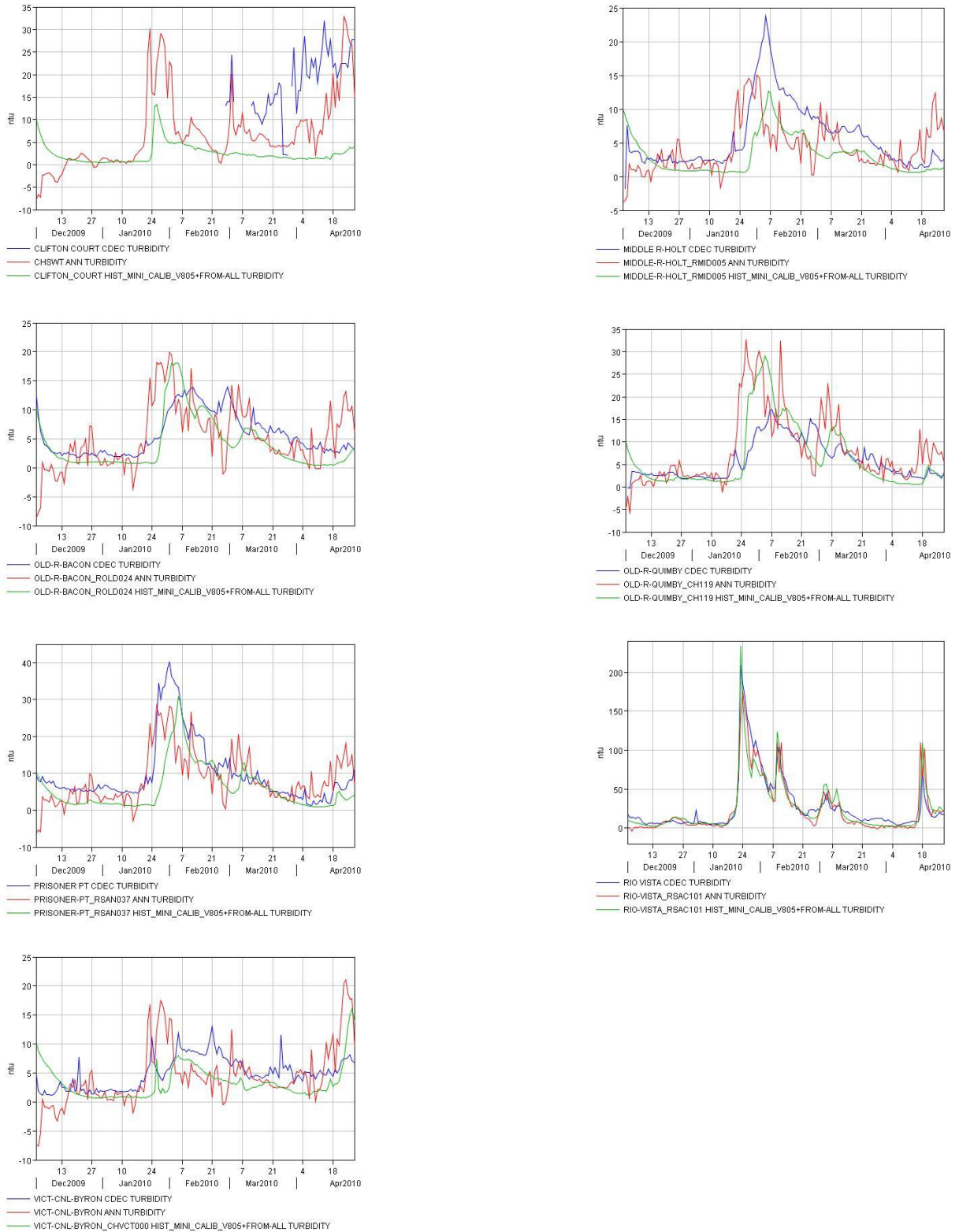


Figure 3-40 Comparison of ANN simulated turbidity (red) during wet season of 2010 at different locations to observed turbidity from CDEC (blue) and simulated turbidity by DSM2 (green).



## 4 SUMMARY AND DISCUSSION

---

This study was planned as an exploration of the application of ANNs to represent turbidity in the Delta, using synthetic data from DSM2. ANNs were selected as the methodology, given the past success of this tool for modeling salinity in prior work performed by DWR. The present evaluation of ANNs for turbidity (termed Phase 1) forms a basis for further development, where the methodology may be applied to a greater number of stations and with a wider range of boundary inputs.

The results presented in the preceding chapter show that the ANN methodology was quite successful at representing turbidity at various locations in the Delta. Specifically, using boundary values of flow and turbidity alone, a single model ANN was able to capture the variation of turbidity at seven locations tested. The quality of the fit was improved substantially when the model was used to evaluate performance on a monthly, as opposed to a daily, basis. Further testing using separate ANN models for each output location showed a modest improvement in fit, but the improvement was not large enough to justify the additional complexity of building seven separate models. The ANN modeling was also applied using a tidal term in the input and showed minimal improvements in the fits. The use of a recurrent (or feedback) network, NARX, where predictions were based on boundary values of flow and turbidity as well as turbidity values at the output locations, was greatly improved over the feed-forward network in the situation where the DSM2 values were used for training. This suggests that ANNs trained with data on turbidity at preceding time-steps may be helpful for further improving the quality of the fit at short time scales. For longer time scales, as might be used in planning applications within CalSim, the feed-forward network may be the best option to use. Overall, these results provide confidence that the ANN methodology is promising as a predictive tool in the Delta for turbidity over the coming years as part of the management framework needed to address the needs that arise from the Delta smelt Biological Opinion.

The Matlab programming environment used for the ANN development also allows for export of a trained network into a stand-alone application. An application for the single network trained ANN is provided as part of this Phase 1 process. This application runs

from a command prompt, and uses Excel files for input and output. This is a basic interface and will be enhanced in a future phase of this work.

Despite the overall success of the ANN approach, some caveats must be noted. The ANN is fit to DSM2 simulated values of turbidity and not to real data. Until further validation of the DSM2 turbidity model is performed, it cannot be ascertained if the ANN can always predict turbidity in the real-world. Preliminary evaluation of the trained ANN against real data (not DSM2 output) show that the ANN does well in locations where DSM2 does well at capturing real-world behavior, although there are locations both the ANN and DSM2 fits are not very good. Continued calibration and evaluation of the DSM2 model as well as continued testing and development of the ANN using observed data will help to address this gap. The existing network of turbidity stations with frequent measurements of turbidity (every 15 minutes) provides a basis for this continued development. Also, preliminary testing of the trained ANN showed that performance of the model was not robust when inputs in excess of the training range were used. This is a typical feature of empirical, data-driven models, and in this case needs to be addressed through pre-processing of the input files.

## 5 REFERENCES

---

Armor, C.S., and T.R. Sommer. 2006. Pelagic organism decline 2005–2006: overview of program and progress, 4<sup>th</sup> Biennial CALFED Science Conference 2006, October 23–25, 2006, Sacramento Convention Center.

Beale, M.H., M.T. Hagan, H.B. Demuth. 2011. Neural Network Toolbox. User's Guide.

California Department of Water Resources. 2002. DSM2 tutorial. An introduction to the Delta Simulation Model II (DSM2) for simulation of hydrodynamics and water quality of the Sacramento–San Joaquin Delta. February 2002.

Demuth, H., M. Beale. 2002. Neural Network Toolbox for Use with Matlab. User's Guide, Version 4.

Finch, R. and N. Sandhu. 1995. Artificial neural networks with application to the Sacramento–San Joaquin Delta. California Department of Water Resources, Delta Modeling Section, Division of Planning.

Hutton, P. 2008. A model to estimate combined Old and Middle River flows. Metropolitan Water District of Southern California. April 2008.

Liu, L., P. Sandhu. 2011. Chapter 7: Turbidity modeling with DSM2. In methodology for flow and salinity estimates in the Sacramento–San Joaquin Delta and Suisun Marsh. 32<sup>nd</sup> Annual Progress Report. June 2011.

Maier, H.R., G.C. Dandy. 2000. Neural networks for the prediction and forecasting of water resources variables: a review of modeling issues and applications. *Environmental Modeling and Software* 15: 101–124.

Maier, H.R., A. Jain, G.C. Dandy, K.P. Sudheer. 2010. Methods used for the development of neural networks for the prediction of water resource variables in river

systems: current status and future directions. *Environmental Modeling and Software* 25: 891–909.

Resource Management Associates (RMA). 2008. Sacramento–San Joaquin Delta Turbidity Modeling, Technical Memorandum prepared for the Metropolitan Water District of California.

Resource Management Associates (RMA). 2010. Turbidity and adult delta smelt forecasting with RMA 2-D models: December 2009–May 2010. Report prepared for Metropolitan Water District of Southern California.

Sandhu, N., D. Wilson, and R. Finch. 1999. Modeling flow-salinity relationships in the Sacramento–San Joaquin Delta using artificial neural networks. Technical Information Record OSP-99-1. California Department of Water Resources. Sacramento, CA.

Seneviratne, S., S. Wu, and Y. Liang. 2008 Chapter 3: Impacts of sea level rise and amplitude change on Delta operations. Methodology for flow and salinity estimates in the Sacramento–San Joaquin Delta and Suisun Marsh. 29th Annual progress report. June 2008.

Smith, P.E., C.A. Ruhl, and J. Simi (2006). Hydrodynamic Influences on Historical Patterns in Delta Smelt Salvage, 4th Biennial CALFED Science Conference 2006, October 23–25, 2006, Sacramento Convention Center.

Wilbur, R. and A. Munevar. 2001. Chapter 7: Integration of CalSim and Artificial Neural Networks models for Sacramento–San Joaquin Delta flow-salinity relationships. In Methodology for flow and salinity estimates in the Sacramento–San Joaquin Delta and Suisun Marsh. 22<sup>nd</sup> Annual Progress Report. August 2001.

# APPENDIX A: FLOW-TURBIDITY RELATIONSHIPS AT BOUNDARY LOCATIONS

---

## SACRAMENTO RIVER AT FREEPORT

Define three flow-turbidity relationships that are approximately based on an RMA analysis of suspended sediment data (see Table 4-7 in RMA, 2010). Assume linear interpolation to provide continuous turbidity values as a function of flow.

Flow Range cfs	Low (50%)	Mid (75%)	High (90%)
< 10,000	10	15	20
12,500	20	30	40
17,500	30	40	70
22,500	40	60	100
27,500	60	100	160
32,500	70	140	280
37,500	90	160	<b>320</b>
45,000	100	170	350
55,000	100	175	300
65,000	<b>100</b>	140	240
>70,000	100	140	180

## SAN JOAQUIN RIVER AT VERNALIS

Define two flow-turbidity relationships that are loosely based on an RMA analysis of suspended sediment data (see Table 4-8 in RMA, 2010). Assume linear interpolation to provide continuous turbidity values as a function of flow.

Flow Range cfs	Low (50%)	High
<2,000	15	100
2,750	20	100
4,250	25	100
7,500	25	90
15,000	20	60
>20,000	15	60

## YOLO BYPASS

Define three flow-turbidity relationships that are loosely based on an RMA analysis (see Table 5-2 in RMA, 2010). Assume linear interpolation to provide continuous turbidity values as a function of flow.

Flow Range cfs	Low	Mid	High
<100	20	20	20
1,000	30	40	60
5,000	60	120	200
10,000	100	200	300
>30,000	100	150	200

## COSUMNES RIVER

Define three flow-turbidity relationships that are loosely based on an RMA analysis (see Table 4-5 in RMA, 2010) and a WARMF model historical simulation of water years 2002–2011. Assume linear interpolation to provide continuous turbidity values as a function of flow.

Flow Range cfs	Low	Mid	High
<100	10	10	10
500	30	50	80
1,000	50	100	180
2,000	80	200	280
>3,000	100	300	300

## MOKELUMNE RIVER

Define the following flow-turbidity relationship that is loosely based on an RMA analysis (see Table 4-5 in RMA, 2010). Assume linear interpolation to provide continuous turbidity values as a function of flow.

Flow Range cfs	Low	Mid	High
<100	20	20	20
500	30	50	80
>1,000	40	70	100

## CALAVERAS RIVER

Define three flow-turbidity relationships that are loosely based on an RMA analysis (see Table 4-5 in RMA, 2010) and a WARMF model historical simulation of water years 2002–2011. Assume linear interpolation to provide continuous turbidity values as a function of flow.

Flow Range cfs	Low	Mid	High
<50	20	20	20
100	30	30	40
>1,000	40	70	100



# APPENDIX B: COMPARISON OF DSM2 OUTPUT TO REAL-TIME TURBIDITY DATA COLLECTED IN THE DELTA

---

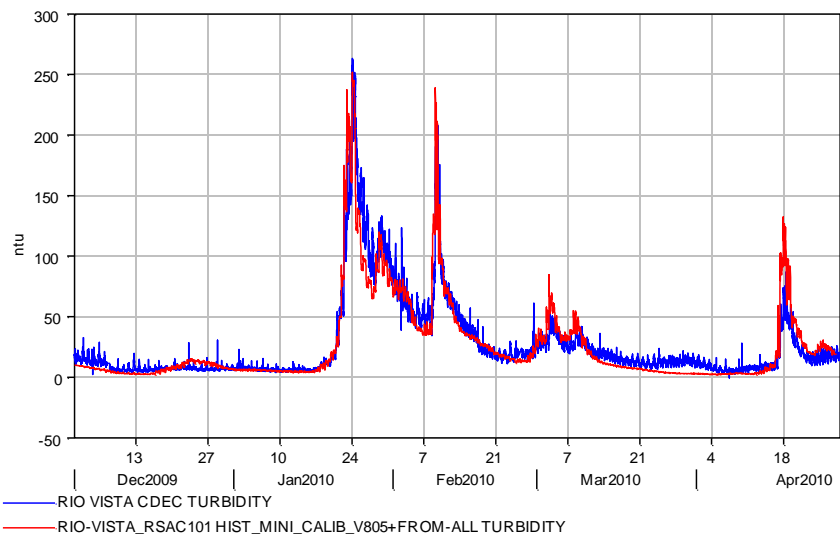


Figure B-1 DSM2 simulated turbidity (red) and observed turbidity from CDEC (blue) at Sacramento River at Rio Vista.

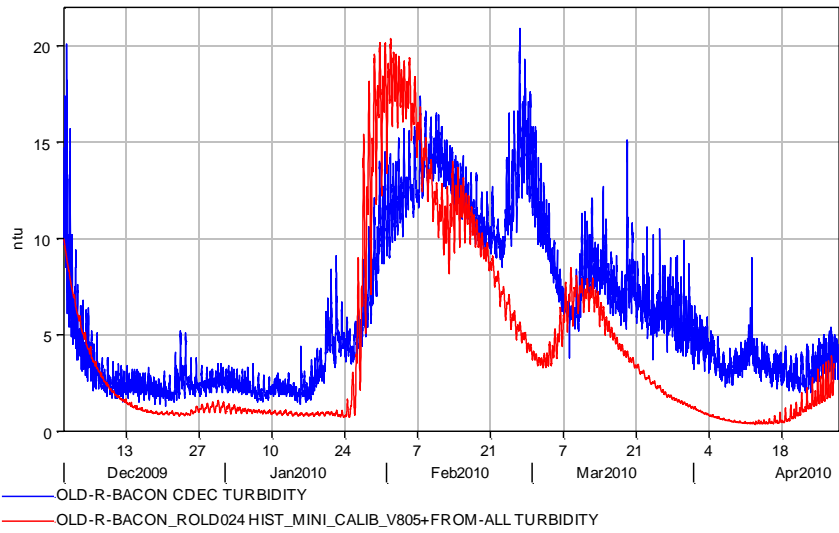


Figure B-2 DSM2 simulated turbidity (red) and observed turbidity from CDEC (blue) at Old River Bacon Island.

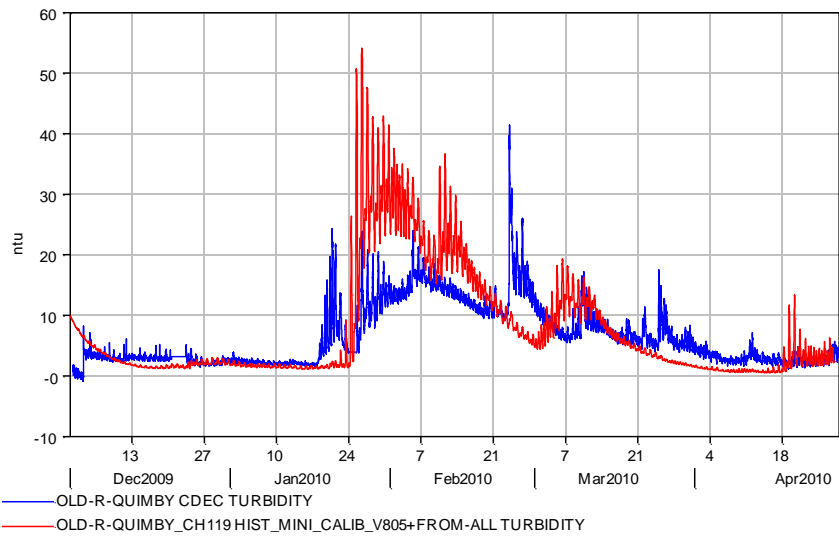


Figure B-3 DSM2 simulated turbidity (red) and observed turbidity from CDEC (blue) at Old River Quimby Island.

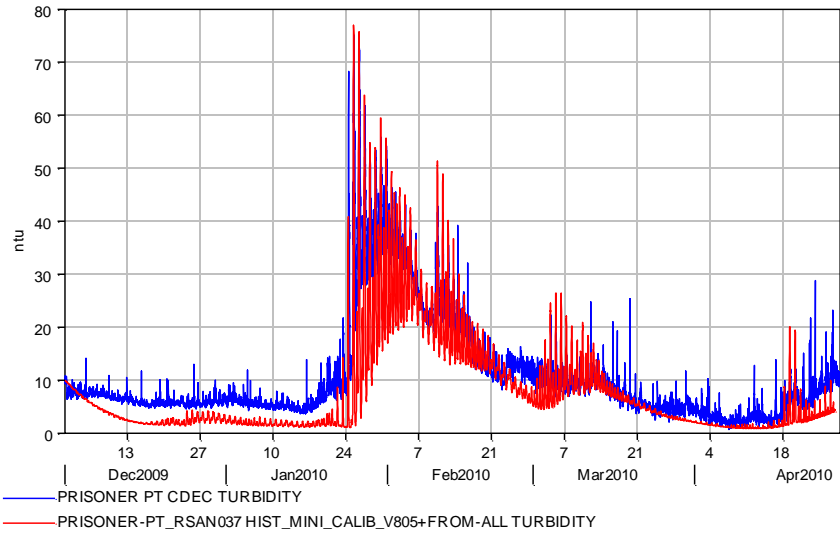


Figure B-4 DSM2 simulated turbidity (red) and observed turbidity from CDEC (blue) at San Joaquin River at Prisoners Point.

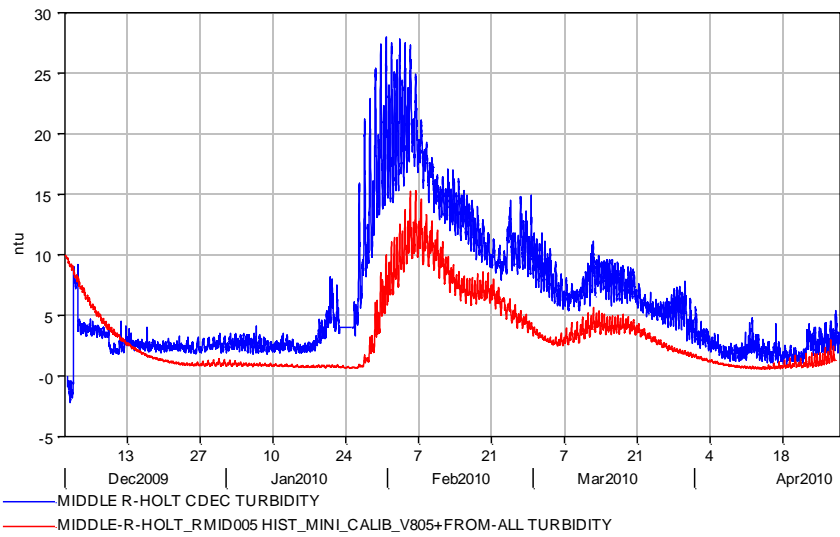


Figure B-5 DSM2 simulated turbidity (red) and observed turbidity from CDEC (blue) at Middle River at Holt.

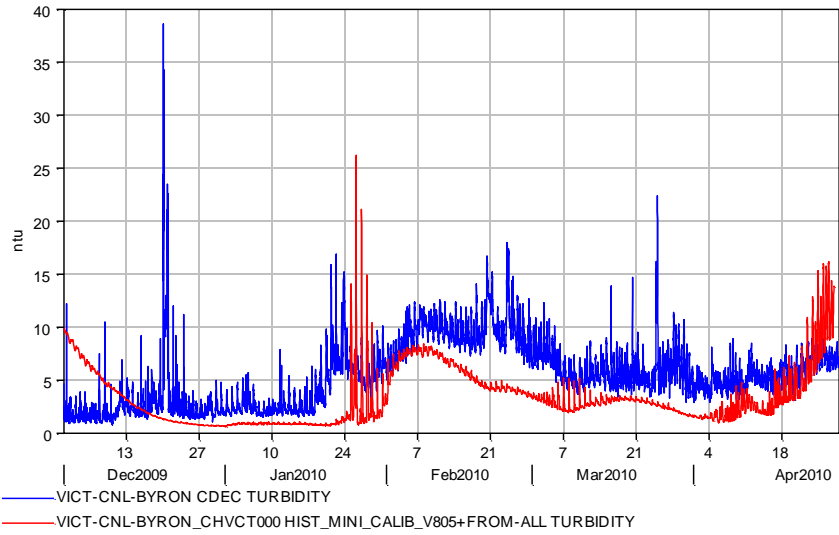


Figure B-6 DSM2 simulated turbidity (red) and observed turbidity from CDEC (blue) at Victoria Canal.

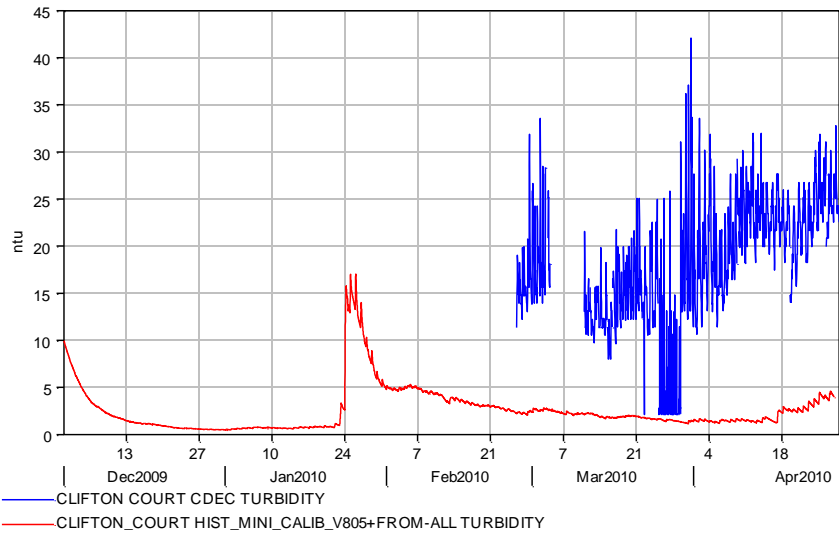
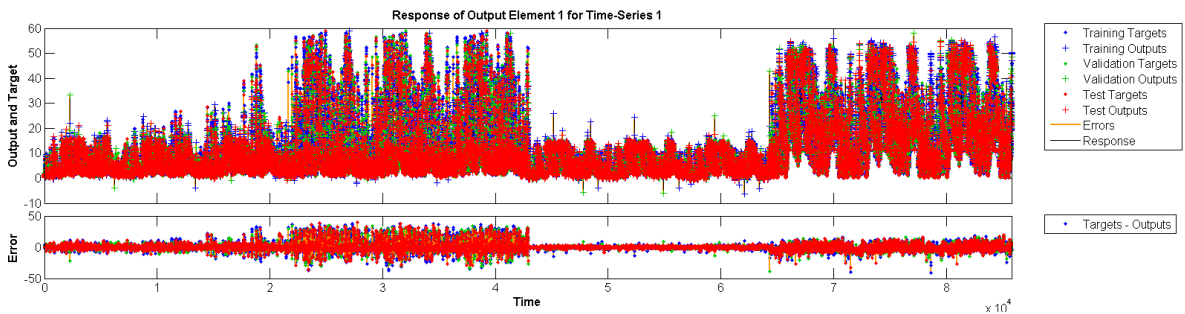


Figure B-7 DSM2 simulated turbidity (red) and observed turbidity from CDEC (blue) at Clifton Court.

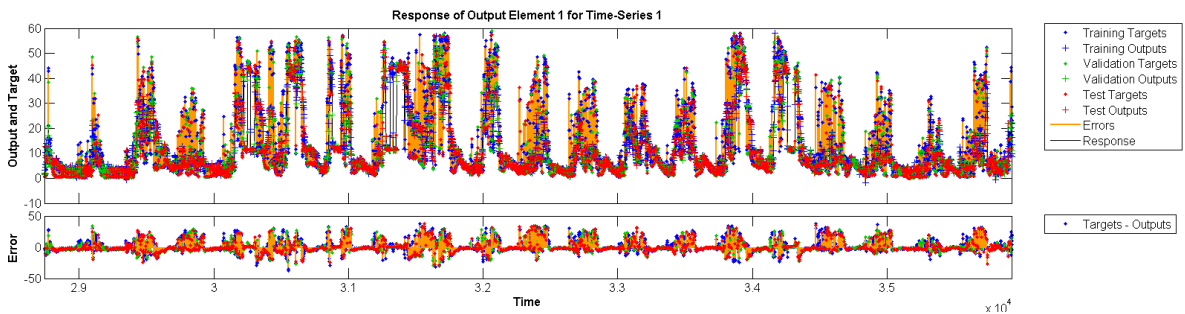
# APPENDIX C: TIME SERIES OF TRAINED AND DSM2 SIMULATED TURBIDITY FOR THE TRAINING, VALIDATION AND TEST DATASETS FOR: A) TWELVE SCENARIOS; B) 20-YEAR; C) 5-YEAR; AND D) 1-YEAR PERIOD OF SCENARIO 5

---

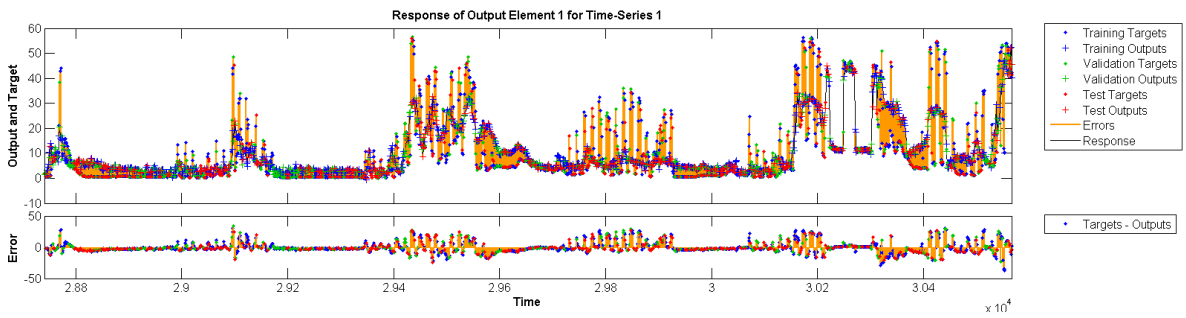
a) Twelve Scenarios



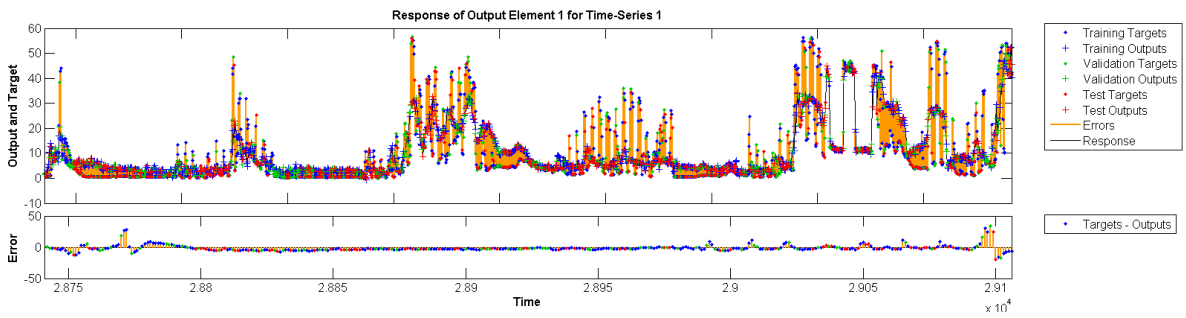
b) 20-year (Scenario 5)



c) 5-year (Scenario 5)



d) 1-year (Scenario 5)



# APPENDIX D: ANN TRAINED TURBIDITY USING 12 SCENARIOS COMPARED TO DSM2 SIMULATED TURBIDITY

